A bispecific gd T-cell engager targeting EGFR activates a potent Vg9Vd2 T cell-mediated immune response against EGFR-expressing tumors

King, L.A.; Toffoli, E.C.; Veth, M.; Iglesias-Guimarais, V.; Slot, M.C.; Amsen, D.; ... ; Vliet, H.J. van der

A Bispecific γδ T-cell Engager Targeting EGFR Activates a Potent Vγ9Vδ2 T cell–Mediated Immune Response against EGFR-Expressing Tumors

Lisa A. King[1,2,3], Elisa C. Toffoli[1,2,3], Myrthe Veth[1,2,3], Victoria Iglesias-Guimarais[4], Manon C. Slot[3,5], Derk Amsen[3,5], Rieneke van de Ven[2,3,6], Sarah Derks[1,2,3], Marieke F. Fransen[2,3,7], Jurriaan B. Tuynman[8], Thilo Riedl[4], Rob C. Roovers[4], Anton E.P. Adang[4], Jurjen M. Ruben[4], Paul W.H.I. Parren[4,9], Tanja D. de Gruijl[1,2,3], and Hans J. van der Vliet[1,2,4]

ABSTRACT

Vγ9Vδ2 T cells are effector cells with proven antitumor efficacy against a broad range of cancers. This study aimed to assess the antitumor activity and safety of a bispecific antibody directing Vγ9Vδ2 T cells to EGFR-expressing tumors. An EGFR-Vδ2 bispecific T-cell engager (bsTCE) was generated, and its capacity to activate Vγ9Vδ2 T cells and trigger antitumor activity was tested in multiple *in vitro*, *in vivo*, and *ex vivo* models. Studies to explore safety were conducted using cross-reactive surrogate engagers in nonhuman primates (NHP). We found that Vγ9Vδ2 T cells from peripheral blood and tumor specimens of patients with $EGFR^+$ cancers had a distinct immune checkpoint expression profile characterized by low levels of PD-1, LAG-3, and TIM-3. Vγ9Vδ2 T cells could be activated by EGFR-Vδ2 bsTCEs to mediate lysis of various $EGFR^+$ patient–derived tumor samples, and substantial tumor growth inhibition and improved survival were observed in *in vivo* xenograft mouse models using peripheral blood mononuclear cells (PBMC) as effector cells. EGFR-Vδ2 bsTCEs exerted preferential activity toward $EGFR^+$ tumor cells and induced downstream activation of $CD4^+$ and $CD8^+$ T cells and natural killer (NK) cells without concomitant activation of suppressive regulatory T cells observed with EGFR-CD3 bsTCEs. Administration of fully cross-reactive and half-life extended surrogate engagers to NHPs did not trigger signals in the safety parameters that were assessed. Considering the effector and immune-activating properties of Vγ9Vδ2 T cells, the preclinical efficacy data and acceptable safety profile reported here provide a solid basis for testing EGFR-Vδ2 bsTCEs in patients with $EGFR^+$ malignancies.

Introduction

γδ T cells represent a unique unconventional T-cell population at the interface of innate and adaptive immunity (1). Vγ9Vδ2 T cells are the largest γδ T-cell subset in peripheral blood (PB), accounting for ∼1% to 5% of the total T-cell population, and they recognize target cells in an HLA-independent fashion. They do so by sensing conformational changes in butyrophilin 3A1 (BTN3A1) upon binding of phosphoantigens, such as the mevalonate pathway intermediate isopentenyl diphosphate, to a BTN3A1 intracellular domain (2). Recently, BTN2A1 was identified as an important coreceptor for phosphoantigen-mediated engagement of Vγ9Vδ2 T cells (3). Phosphoantigen-mediated activation of Vγ9Vδ2 T cells stimulates expansion, their capacity to serve as antigen-presenting cells (APC), the production of proinflammatory cytokines and chemokines, and cytotoxicity (4–6). Other receptors, such as NKG2D, can act as costimulatory receptors to support Vγ9Vδ2 T-cell activation against tumor cells by binding to MIC-A/B and ULBPs (7).

Transcriptomic signatures of 18,000 tumors showed that the presence of γδ T cells among tumor-infiltrating immune cells was most significantly associated with favorable prognosis (8). Additional studies confirmed the positive association between Vγ9Vδ2 T-cell infiltration and clinical outcome and reported on the relative abundance of tumor-infiltrating Vγ9Vδ2 T cells in different cancers (9, 10). Together with the demonstration that Vγ9Vδ2 T cells can exert strong cytolytic activity against a wide range of malignancies (11, 12), this has stimulated the development of Vγ9Vδ2 T cell–based cancer immunotherapy clinical trials. These trials included testing systemic activation of Vγ9Vδ2 T cells using amino-bisphosphonates and synthetic phosphoantigens and systemic administration of autologous or allogeneic *ex vivo*–expanded Vγ9Vδ2 T cells, reviewed in (13). Although these studies demonstrated Vγ9Vδ2 T cell–directed therapies to have an acceptable safety profile, clinically relevant antitumor responses were observed only in a minority of cases. Strategies that enhance activation of Vγ9Vδ2 T cells specifically in the tumor microenvironment, e.g., using chimeric antigen receptor (CAR) or bispecific antibody–based approaches, may result in more consistent and robust anticancer activity (13).

Bispecific T-cell engagers (bsTCE) offer "off-the-shelf" immunotherapies and most commonly induce signaling via the CD3–TCR complex upon binding to a target protein on tumor cells, thereby

[1]Department of Medical Oncology, Amsterdam UMC, Vrije Universiteit Amsterdam, Amsterdam, the Netherlands. [2]Cancer Center Amsterdam, Amsterdam, the Netherlands. [3]Amsterdam Institute for Infection and Immunity, Amsterdam, the Netherlands. [4]Lava Therapeutics NV, Utrecht, the Netherlands. [5]Department of Hematopoiesis, Sanquin Research and Landsteiner Laboratory, Amsterdam UMC, University of Amsterdam, Amsterdam, the Netherlands. [6]Department of Otolaryngology and Head and Neck Surgery, Amsterdam UMC, Vrije Universiteit Amsterdam, the Netherlands. [7]Department of Pulmonary Diseases, Amsterdam UMC, Vrije Universiteit Amsterdam, the Netherlands. [8]Department of Surgery, Amsterdam UMC, Vrije Universiteit Amsterdam, Amsterdam, the Netherlands. [9]Department of Immunology, Leiden University Medical Center, Leiden, the Netherlands.

Corresponding Author: Hans J. van der Vliet, Yalelaan 60, 3584 CM, Utrecht, the Netherlands. Phone: 31-020-4445152; E-mail: h.vandervliet@lavatherapeutics.com; and De Boelelaan 1117, 1081 HV, Amsterdam, the Netherlands. E-mail: jj.vandervliet@amsterdamumc.nl

Cancer Immunol Res 2023;11:1237–52

doi: 10.1158/2326-6066.CIR-23-0189

triggering T cell–mediated tumor lysis (14). Although impressive clinical results have been obtained with CD3-targeting bsTCE (e.g., blinatumomab) in B-cell malignancies, toxicities such as cytokine release syndrome (CRS) and immune effector cell–associated neurotoxicity syndrome often occur, and broadening of the use of bsTCE, specifically to solid tumors, has been challenging (15). Moreover, concomitant engagement of regulatory T cells (Treg) by CD3-targeting bsTCE negatively affects clinical outcome (16). Engaging innate like T-cell subsets with inherent antitumor activity, like Vγ9Vδ2 T cells, has the potential to overcome these challenges and could combine high therapeutic efficacy with a reduced risk of CRS and off-tumor toxicity.

We have developed bispecific single-domain antibodies (VHH, variable fragment of a heavy chain–only antibody) that activate Vγ9Vδ2 T cells to selectively kill $EGFR^+$ tumor cells. Here, we extend our earlier findings (17) using a different Vδ2-specific VHH, and advance our concept toward the clinic by demonstrating that Vγ9Vδ2 T cells, present in both patient PB and $EGFR^+$ tumor specimens, could be activated by EGFR-Vδ2 bsTCEs to kill autologous patient-derived tumor cells and trigger Vγ9Vδ2 T cells in peripheral blood mononuclear cells (PBMC) to control tumor growth in an *in vivo* mouse model. Analysis of cancer-associated Vγ9Vδ2 T cells showed them to be versatile effector cells, expressing low levels of inhibitory immune-checkpoint receptors. EGFR-Vδ2 bsTCE–mediated activation of Vγ9Vδ2 T cells triggered subsequent IFNγ- and TNF-mediated downstream activation of T and natural killer (NK) cells, and avoided the coactivation of suppressive Tregs that was observed with EGFR-CD3 bsTCE. Finally, as severe toxicity was reported for EGFR-CD3 bsTCEs in nonhuman primates (NHP; ref. 18), we additionally explored the anticipated safety profile of our approach in NHP and found no clinical, biochemical, or histopathologic signs of toxicity, including no CRS, despite demonstrable target engagement.

Materials and Methods

Tumor cell lines

A431 (CRL-1555), $SW480^{KRAS\text{-}G12V}$ (CCL-228), $HT\text{-}29^{BRAF\text{-}V600E}$ (HTB-38), and $HCT\text{-}116^{KRAS\text{-}G13D}$ (CCL-247) were obtained from ATCC between 2017 and 2021. COLO320 and WiDr were previously described and maintained in our institute (17, 19). Tumor cell lines were maintained in DMEM (41965-039, Gibco) supplemented with 10% (v/v) fetal calf serum (FCS, 04-007-1A, Biological Industries), 0.05 mmol/L 2-mercaptoethanol (200-646-6, Merck), 100 IU/mL sodium penicillin, 100 μg/mL streptomycin sulfate, and 2.0 mmol/L L-glutamine (PSG, 10378-016, Life Technologies) and kept at 37°C in a humidified atmosphere containing 5% CO_2. As cell lines were obtained directly from ATCC and only early cell line passages (5–14) were used, in-house characterization was limited to confirmation of EGFR expression. Cell lines were tested for *Mycoplasma* using PCR every 3 months.

Patient tissue samples, PBMC isolation, and lymphocyte culture

PBMCs were isolated from whole blood using Lymphoprep (AXI-1114547, Fresenius) density gradient centrifugation. The PBMCs were collected from healthy donors ($n = 31$, Sanquin) and cancer patients (Amsterdam UMC). Cancer patient tissue ($n = 77$, i.e., primary and metastatic malignant and nonmalignant tissues derived from colon, peritoneum, liver, lung, esophagus, and head and neck) was surgically collected (endoscopically for esophageal samples) and processed at the Amsterdam UMC (location VUmc). PBMCs and tissue samples were obtained after written informed consent was obtained (patient characteristics; Supplementary Table S1). The study was approved by the medical ethics committee at the Amsterdam UMC and conducted in accordance with the Declaration of Helsinki. Tissue was cut into small pieces, resuspended in IMDM (12440061, Gibco) supplemented with 0.1% DNAse I (10104159001, Roche), 0.14% Collagenase A (10103586001, Roche), 5% FCS and PSG, and stirred in a flask for 45 minutes at 37°C. Cells were processed immediately for flow cytometry and/or used for functional experiments. Vγ9Vδ2 T and invariant NK T (iNKT) cells were isolated from healthy donor PBMC and expanded as described (20, 21); purity for experiments was >95%.

Cynomolgus monkey PBMC (CITox) were cultured in RPMI medium (22400–089, Gibco) supplemented with 10% FCS, 0.05 mmol/L 2-mercaptoethanol, PSG, 10 μmol/L zoledronic acid (SML0223, Sigma), and 100 U/mL IL2 (Novartis) for 7 days to expand $V\gamma9^+$ T cells.

Tregs derived from healthy donor PBMCs were isolated based on a $CD25^+CD127^-GPA33^+$ phenotype and expanded as described (22).

Flow cytometry

Tissue single-cell suspensions, PBMC, expanded Vγ9Vδ2 T and iNKT cells, and tumor cells were resuspended in PBS (1073508600, Fresenius Kabi) supplemented with 0.5% bovine serum albumin (M090001/03, Fisher Scientific) and 20 μg/mL NaN_3 (247-852-1, Merck) and incubated with fluorochome-labeled mAbs (Supplementary Table S2) for 30 minutes at 4°C. Measurement was done using the LSRFortessa XL-20 (BD). Data were analyzed using Kaluza Analysis v1.3 (Beckman Coulter) or FlowJo v10.7.2 (BD). Cytometric bead array (CBA) data were analyzed with FCAP Array software v3.0 (BD).

Generation and assessment of target binding of bispecific antibodies

The following bsTCEs were generated: EGFR-Vδ2 bsTCE, EGFR-CD3 bispecific T-cell engager (BiTE), EGFR-Vγ9 bsTCE, EGFR-Vγ9-Fc bsTCE, and EGFR-Vδ2-Fc bsTCE (Supplementary Fig. S1 provides a schematic overview of the bcTCEs, and a detailed characterization of the bsTCEs is provided in the Results section in this publication). The EGFR-Vδ2 bsTCE was generated by linking EGFR-specific VHH7D12 (23) N-terminally to Vδ2-TCR-specific VHH5C8 (24) using a Gly_4Ser sequence (VHH-(G4S)-VHH). The EGFR-Vδ2-Fc bsTCE was generated by linking the VHHs to an Fc domain as outlined below. EGFR-CD3 BiTE was generated by linking the scFv of EGFR-specific mAb clone 225 (25) N-terminally to CD3ε-specific mAb clone TR66 (18) using a Gly_4Ser sequence and hexahistidine tagged for purification (VL-$(G4S)_3$-VH-AA(G4S)-VH-(VEGGSGGSGGSGGSGGVD)-VL). Purified protein was produced by ImmunoPrecise Antibodies (IPA) using DNA transfected HEK293E cells and rmp-Protein-A affinity chromatography (EGFR-Vδ2 bsTCE) or immobilized metal affinity chromatography (IMAC; EGFR-CD3 BiTE) and preparative size-exclusion chromatography. Binding to Vδ2, CD3, and EGFR was determined by incubating target cells with EGFR-Vδ2 bsTCE or EGFR-CD3 BiTE (45 minutes, 4°C), washing, incubation (30 minutes, 4°C) with FITC-labeled anti-llama polyclonal Abs (EGFR-Vδ2 bsTCE), or PE-labeled anti–his-tag Abs (EGFR-CD3 BiTE) and flow cytometry (see Supplementary Table S2 for the antibody information).

Two EGFR-Vγ9 bsTCEs were generated. One, an EGFR-Vγ9 bsTCE, where a Gly_4Ser sequence links the EGFR-specific VHH-7D12 (ref. 23; cross-reactive for human and cynomolgus EGFR, ref. 26) to the scFv of Vγ9-specific mAb [clone 7A5, sequence provided by Prof. D. Kabelitz (University of Kiel, Germany), cross-reactive for human and cynomolgus Vγ9; VHH-(G4S)-VL-$(G4S)_4$-VH] at the C-terminus (27). The other, an EGFR-Vγ9-Fc bsTCE, is a half-life extended construct containing the same EGFR-specific

VHH-7D12 (HC2, VHH-hinge-Fc) and Vγ9-specific scFv [HC1, VL-$(G4S)_4$-VH-hinge-Fc] now linked to an Fc domain with knobs-into-hole technology for heterodimerization (ref. 28; HC1, knob mutation T366W and HC2, hole mutations T366S, L368A, and Y407V), LFLE mutations to silence the Fc domain [L234F and L235E silencing (EU numbering)], a Cys220 deletion to avoid an unpaired cysteine and a slightly modified hinge (29). EGFR-Vγ9 bsTCEs were purified using protein A affinity chromatography and preparative size exclusion (IPA). Proteins used were >95% pure and monomeric; native MS analysis showed >94% heterodimer. Binding of EGFR-Vγ9 bsTCE (biotinylated with NHS-D-biotin, Sigma-Aldrich) to cynomolgus Vγ9 T cells was assessed using APC-labeled streptavidin and flow cytometry, while binding to cynomolgus EGFR was detected by ELISA. For the ELISA, wells of a clear bottom F96-well Maxisorp plate (#439454, Nunc) were coated overnight with recombinant cynomolgus EGFR (10 μg/mL, 90285-C08B, SinoBiological). Wells were blocked with 2% BSA (#A2153, Sigma) for 60 minutes, and test samples were incubated for 120 minutes at RT. The rabbit anti-camelid VHH cocktail (60-minute incubation, 19L002038, GenScript) and swine anti-rabbit immunoglobulins HRP (60-minute incubation, 41289300, Dako) were used for detection and 3,3′,5,5′-Tetramethylbenzidine (TMB, Life Technologies, #SB02) was used as a substrate for color development. The absorbance (450 nm) was measured using a plate reader (Molecular Devices, iD5) and the data analysis was done using SoftMax Pro software v 7.1. Binding of the EGFR-Vγ9-Fc bsTCE to cynomolgus Vγ9 and EGFR was determined using biotinylated (EZ-link Sulfo-NHS-Biotin, 21217, Thermo Fisher) recombinant cynomolgus Vγ9Vδ2-TCR (IPA) and cynomolgus EGFR (10366-ER-100, R&D Systems) in combination with the Octet-based Bio-Layer Interferometry platform (Sartorius).

Assessment of Vγ9Vδ2 T-cell and lymphocyte activation and degranulation

Functional experiments were performed in RPMI medium supplemented with 10% FCS, 0.05 mmol/L 2-mercaptoethanol and PSG. Vγ9Vδ2 T-cell activation was assessed by incubating healthy donor–derived expanded Vγ9Vδ2 T cells with A431, SW480, HT-29, HCT-116, or WiDr cells (1:1 E:T ratio), and/or healthy donor–derived expanded Tregs (1:1:1 E:T ratio) or cancer patient–dissociated tissue suspensions ± indicated concentrations of EGFR-Vδ2 bsTCE or EGFR-CD3 BiTE. Supernatants were stored at −20°C and analyzed using the human $T_H1/T_H2/T_H17$ CBA kit (560484, BD) and granzyme-B, CCL5, CXCL10, and CXCL11 flex--sets (560304, 558324, 558280, 560364, BD). Flow cytometry was used to assess degranulation in the presence of PE-labeled anti-CD107a after 4 or 24 hours and CD25 expression after 24 hours. For blocking experiments, Vγ9Vδ2 T were preincubated 30 minutes with 10 μg/mL Fc-receptor block (130-059-901, Miltenyi Biotec) or anti-NKG2D (MAB139-SP, R&D Systems) and WiDr cells were preincubated 30 minutes with 10 μg/mL cetuximab (Merck) and/or anti-CD277/BTN3A (PABL-415, Creative Biolabs). Activation of human and NHP Vγ9Vδ2 T cells by EGFR-Vδ2 bsTCE or EGFR-Vγ9 bsTCE was assessed after a 24-hour culture with A431 cells (1:1 E:T ratio) or overnight precoated recombinant cynomolgus EGFR (10 μg/mL, Sino Biological) in the presence of anti-CD107a using flow cytometry.

Activation of activated or resting Tregs (FoxP3^{++}CD45RA$^-$ or FoxP3$^+$CD45RA$^+$; ref. 30) was assessed in single-cell suspensions from peritoneal metastases of colorectal cancer patients cultured for 48 hours ± 50 nmol/L EGFR-Vδ2 bsTCE or EGFR-CD3 BiTEs using flow cytometry.

In 7-day cocultures of healthy donor or cancer patient PBMCs and SW480 tumor cells (10:1 E:T ratio) or autologous tumor cells ± 50 nmol/L EGFR-Vδ2 bsTCE, activation of Vγ9Vδ2 T, conventional T, and NK cells was determined by assessing CD25 expression using flow cytometry. Cultures were performed in the presence and absence of 10 μg/mL TNF-specific (MAB2101, R&D Systems) and/or IFNγ-specific (MAB285–100, R&D Systems) neutralizing antibodies or isotype control (401504, BioLegend).

Assessment of target cell lysis

Tumor lysis was assessed by incubating Vγ9Vδ2 T with A431, SW480, HT-29, HCT-116, or WiDr cells or cancer patient tissue–derived single-cell suspensions (1:1 E:T ratio) ± a concentration range or 50 nmol/L of EGFR-Vδ2 bsTCE, EGFR-CD3 BiTE, or EGFR-Vγ9 bsTCE for 4 or 24 hours as indicated. Adhered cells were detached using trypsin-EDTA (15400-054, Gibco), and tumor lysis was determined using 7AAD (A9400-1MG, Sigma) and 123counting eBeads (01-1234-42, Thermo Fisher) followed by flow-cytometry analysis.

SW480 tumor lysis was also assessed in 7-day cultures with healthy donor or cancer patient PBMCs (metastatic colorectal cancer or primary esophageal cancer; 10:1 E:T ratio) ± 50 nmol/L EGFR-Vδ2 bsTCE. Where indicated, SW480 cells were preincubated for 30 minutes with 10 μg/mL HLA-I–specific (MA1-19027, Thermo Fisher) or HLA-II–specific blocking antibodies (555557, BD) or isotype control (401504, BioLegend) and Vδ2$^+$, CD4$^+$, CD8α$^+$, CD8β$^+$, or CD56$^+$ cells were MACS-depleted from PBMCs using population-specific mAbs and goat anti-mouse IgG microbeads (130-048-401, Miltenyi Biotec).

Autologous patient tumor cell lysis (tumor cells were identified as EpCAM$^{+/dim}$CD45$^-$ cells, and lysis was quantified using 7AAD and 123counting eBeads) was assessed (using flow cytometry) by coculturing colorectal cancer patient PBMCs or MACS-purified (CD3 REAlease kit, 130-121-562; Miltenyi Biotec) tumor-infiltrating T-cell fractions (purity >80%) enriched from primary or peritoneal metastatic colorectal cancer single-cell suspensions with matched patient tumor cells ± 50 nmol/L EGFR-Vδ2 bsTCE for 24 hours (tumor-infiltrating T cells; 1:1 E:T ratio) or 7 days (PBMC; 5:1 E:T ratio).

In vivo mouse studies

For *in vivo* mouse studies, female immunodeficient NOD–scid *Il2rg*$^{-/-}$ (NPG) mice (6–7 weeks) that were kept under pathogen-free conditions were used (Crown Bioscience). In the HCT-116 study, mice were randomized into 4 groups ($n = 8$/group) and subcutaneously (s.c.) inoculated with 5×10^6 HCT-116 tumor cells alone or admixed with 5×10^6 PBMCs of either of 2 healthy donors in a 1:1 E:T ratio. PBS or EGFR-Vδ2 bsTCE (0.5 or 5.0 mg/kg) was intravenously (i.v.) administered daily for 14 days. In the A431 study, mice were s.c. inoculated with 5×10^6 A431 tumor cells admixed with 5×10^6 PBMCs of 1 healthy donor in a 1:1 E:T ratio and treated weekly (starting day 0) with i.v. PBS or 2 mg/kg half-life extended EGFR-Vδ2-Fc bsTCE ($n = 8$/group) preceded (30 minutes earlier) by an intraperitoneal immunoglobulin injection (IVIG, 10 mg/mouse). Mice were checked daily for physiologic parameters and twice weekly for tumor volume using a caliper. Tumor volume was expressed in mm^3 using the formula: $V = (L \times W \times W)/2$, where V was tumor volume, L was tumor length (the longest tumor dimension), and W was tumor width (the longest tumor dimension perpendicular to L). Animals were terminated when tumors reached 2,000 mm^3 or when mandated. The *in vivo* studies were performed at the facility of Crown Bioscience, conducted in accordance with the regulations of the Association for

Assessment and Accreditation of Laboratory Animal Care (AAALAC) and approved by the Institutional Animal Care and Use Committee (IACUC) of Crown Bioscience (Taicang) Inc. (Beijing, China).

NHP studies

Safety, pharmacokinetic and pharmacodynamic effects of targeting Vγ9Vδ2-T cells to EGFR were explored in a total of nine NHP using two fully cross-reactive EGFR-Vγ9 bsTCEs (one VHH-scFv and one Fc-domain containing VHH-scFv format).

The EGFR-Vγ9 bsTCE (VHH-scFv) was tested in 6 female *Macaca fascicularis* [3–5 kg, Crown Bioscience (Taicang) Inc]. This study was approved by Crown Bioscience IACUC, and all procedures related to housing, handling, caring, and treatment of the animals were performed in compliance with the guidelines approved by the AAALAC. Three NHP received a single dose of the EGFR-Vγ9 bsTCE (0.03 mg/kg, 0.1 mg/kg, or 0.3 mg/kg, $n = 1$/dose, 30 minutes i.v.) and three (other) NHP received 7-daily EGFR-Vγ9 bsTCE doses (0.03 mg/kg, 0.1 mg/kg, or 0.3 mg/kg, $n = 1$/dose, 30 minutes i.v.). Venous blood samples were collected predose (days −14 and −7) and at multiple time points thereafter for pharmacokinetics (PK) and flow-cytometry analysis using anti-CD45, CD3, CD4, CD8, CD14, CD20, CD25, CD69, TCR Vγ9, TCR pan-γδ, and anti-VHH Abs. EGFR-Vγ9 bsTCE plasma concentrations were measured using a Simoa-free drug assay (PK Solver software version 2.0) by Active Biomarkers. In multiple dosed animals, complete blood cell count (determined in 1 mL whole blood collected in K2-EDTA BD Vacutainer tubes; 367841), parameters of coagulation (determined in 1.8 mL whole blood Vacuette PREMIUM tubes with 3.8% buffered sodium citrate solution; 454381), liver and kidney function, (pre-)albumin, globulin, uric acid (all determined after collection of 1 to 2 mL of whole blood in BD Vacutainer SST II Plus plastic serum tubes (367957) that were centrifuged at 3,500 rpm for 10 minutes after samples were allowed to clot for a minimum of 30 minutes at room temperature), and cytokines (IL1β, IL2, IL4, IL5, IL6, IL8, IL10, TNF, IFNγ, IL12p70, IL15, CCL2; determined in 0.7 mL blood samples collected in BD Vacutainer K2-EDTA tubes (367841), centrifuged at 3,000 rpm for 10 minutes at 4°C, and transferred into polypropylene screw-cap vials for storage at −80°C until analysis) were also measured. NHP were euthanized 24 hours after the last dose for tissue collection and analyses. Axillary lymph nodes were collected 14 days prior to and 7 days after the first dose for flow cytometry using CD3, TCR-Vγ9, CD25, CD69, and anti-VHH antibodies. EGFR-Vγ9-Fc bsTCE was tested in 3 female *Macaca fascicularis* (3–4 kg, Cynbiose SAS). The study was approved by the Animal Welfare Body of Cynbiose and the Ethics Committee of VetAgro-Sup and performed in compliance with the guidelines approved by the AAALAC. NHP received 4 weekly EGFR-Vγ9-Fc bsTCE infusions (1 mg/kg, 5 mg/kg, and 23 mg/kg, $n = 1$/dose, 30 minutes i.v.). Blood samples were collected predose (days −14 and −7) and at multiple days after infusion for PK and flow cytometry using anti-CD3, TCR Vγ9, TCR pan-γδ, CD25, CD69, and anti-VHH Abs, and assessment of hematologic and biochemical parameters and cytokine levels. EGFR-Vγ9-Fc bsTCE plasma concentrations were measured using ELISA. For the ELISA, wells of a clear bottom F96-well Maxisorp plate (#439454, Nunc) were coated overnight with 0.25 μg/mL human Gamm9Delta2 TCR-Fc fusion protein (UPE, Batch 4927 P1). Wells were blocked with 2% BSA (Sigma, #A2153) for 90 minutes and test samples and standards were incubated for 120 minutes at RT. The rabbit anti-camelid VHH HRP (GenScript, #A01861) was used for detection (incubated for 60 minutes at RT) and 3,3′, 5,5′-Tetramethylbenzidine (TMB, Life Technologies, #SB02) was used as substrate for color development. The absorbance (450 nm) was measured using a plate reader (Molecular Devices, iD5), and the data analysis was done using SoftMax Pro software v 7.1. For curve fitting a fixed weighting 4-Parameter fit was used. NHP were euthanized for tissue collection 24h after the last dose. Tissues from liver, kidney, skin, stomach, small and large intestines, spleen, lymph nodes (axillary, submandibular, mesenteric), muscle, thymus, lungs, bladder, ovary, uterus, and vagina were paraffin-embedded for H&E staining and histopathologic examination. H&E staining was performed according to Cerba Research internal procedures. Slides were digitalized with the Nanozoomer scanner (Version 2.0 HT, Hamamatsu) in bright field mode, with a 20× objective (no z-stack). The histopathologic assessment was carried out on digital H&E-stained slides to determine the presence or absence of side effects from the dispensed treatment. Microscopic findings were graded 0–5 (0, no finding; 1, minimal; 2, mild; 3, moderate; 4, marked; 5, severe) for the different organs. Pieces of skin, muscle, colon, lymph node, and spleen were frozen in optimal cutting temperature (Tissue Tek) compound for EGFR-Vγ9-Fc bsTCE detection using HP-coupled anti-human IgG (2049-05, Southern Biotech) combined with Chromomap DAB and IHC staining for EGFR (clone ICR10, ab231, Abcam) and Vγ9 (clone 7A5). Toxicokinetic parameters of both studies can be found in Supplementary Tables S3 and S4.

Statistics and EC_{50} calculation

GraphPad Prism v9.1.0 (GraphPad Software) was used for statistical analyses. Data were analyzed using paired or unpaired *t* test, one-way ANOVA with Dunnet multiple comparisons test or Mantel–Cox test as appropriate. $P \le 0.05$ was considered significant, and $P > 0.05$ was considered not significant and is not indicated with asterisks. EC_{50} values were calculated using nonlinear regression analysis with GraphPad Software.

Data availability statement

The data generated in this study are available within the article and its supplementary data files. Raw data are available upon request from either L.A. King or the corresponding author.

Results

EGFR-Vδ2 bsTCEs trigger Vγ9Vδ2 T-cell activation and lysis of EGFR-expressing tumor cell lines

An EGFR-Vδ2 bsTCE was generated by linking VHH-5C8, a high-affinity Vδ2-TCR–specific VHH, N-terminally to the EGFR-specific VHH-7D12 (Supplementary Fig. S1).

The EGFR-Vδ2 bsTCE was shown to bind specifically and with low-nanomolar apparent affinity to healthy donor–derived expanded Vγ9Vδ2 T cells and to $EGFR^+$ tumor cells derived from cell lines (**Fig. 1A**). No binding was detected to T cells not expressing the Vγ9Vδ2 TCR (iNKT cells) or the EGFR-negative tumor cell line COLO320, illustrating target specificity. In cocultures of Vγ9Vδ2 T cells and multiple $EGFR^+$ tumor cell lines that differ in EGFR expression levels and KRAS/BRAF mutation status (e.g., A431: $KRAS/BRAF^{wt}$, MFI EGFR: 263.2; HCT-116: $KRAS^{mt}$, MFI EGFR: 159.1; HT-29: $BRAF^{mt}$, MFI EGFR: 26.6; SW480: $KRAS^{mt}$, MFI EGFR: 15.6), the EGFR-Vδ2 bsTCE–induced activation of Vγ9Vδ2 T cells (CD25 upregulation) and their degranulation (CD107a upregulation; **Fig. 1B** and **C**). EGFR-Vδ2 bsTCE–activated Vγ9Vδ2 T cells subsequently triggered tumor lysis regardless of KRAS/BRAF mutational status with an EC_{50} of 8 pmol/L for lysis of A431 cells (**Fig. 1D**).

In 24-hour cocultures of expanded Vγ9Vδ2 T cells and various $EGFR^+$ tumor cell lines, EGFR-Vδ2 bsTCE triggered release of

proinflammatory cytokines IFNγ and TNF and low levels of IL2 and the T_H2 type cytokines IL4 and IL6 (Supplementary Fig. S2A). IL10 and IL17A, cytokines that can exert suppressive and regulatory effects, were not increased or not detected (Supplementary Fig. S2A). We also detected enhanced levels of effector leukocyte attracting chemokines CCL5, CXCL10 and, in A431–Vγ9Vδ2 T-cell cocultures, CXCL11 (Supplementary Fig. S2B).

EGFR-CD3 BiTEs, but not EGFR-Vδ2 bsTCEs, trigger Treg activation, which dampens Vγ9Vδ2 T-effector functions

The ability of EGFR-Vδ2 and EGFR-CD3 bsTCEs to trigger Vγ9Vδ2 T-cell degranulation, EGFR$^+$ tumor cell lysis, and Treg activation was compared. First, binding of the EGFR-CD3 BiTE to EGFR on tumor cells and CD3 on Vγ9Vδ2 T cells was confirmed (Supplementary Fig. S3A). As shown in **Fig. 1E**, EGFR-Vδ2 bsTCEs triggered Vγ9Vδ2 T-cell degranulation at somewhat lower (though not statistically significant) concentrations than EGFR-CD3 BiTEs (EC_{50} 6 vs. 22 pmol/L), though EC_{50}s for tumor lysis were similar (3 vs. 4 pmol/L).

In the tumor microenvironment of patients, EGFR-CD3 BiTEs will not exclusively trigger Vγ9Vδ2 T cells but will also engage other CD3$^+$ T-cell subsets, including Tregs, a highly immunosuppressive T-cell population. To explore whether EGFR-CD3 BiTEs and EGFR-Vδ2 bsTCEs differentially impact Treg activation and effector T-cell responses, healthy donor–derived Tregs (purity >80% CD3$^+$CD4$^+$CD127$^+$CD45RA$^+$CD25$^+$FoxP3$^+$Helios$^+$; ref. 22) were cultured with SW480 tumor cells and healthy donor–derived Vγ9Vδ2 T cells ± EGFR-CD3 BiTEs or EGFR-Vδ2 bsTCEs for 24 hours. In the presence of Tregs, EGFR-CD3 BiTEs induced statistically significantly lower CD107a levels on Vγ9Vδ2 T cells and reduced granzyme-B, IFNγ, TNF, and IL2 secretion compared with EGFR-Vδ2 bsTCEs (**Fig. 1F**). None of these parameters were, however, significantly affected by Tregs when EGFR-Vδ2 bsTCEs were used in cocultures of SW480 tumor cells and Vγ9Vδ2 T cells. In some cases, a minor (not statistically significant) effect could be observed, likely reflecting the mere presence of suppressive Tregs, which may also explain the slight reduction in IL2 levels via consumption of this cytokine by Tregs that constitutively express the high-affinity IL2 receptor. Correspondingly, when tumor cell suspensions of patients with peritoneal colorectal cancer metastases were cultured for 48 hours ± EGFR-CD3 BiTEs or EGFR-Vδ2 bsTCEs, only EGFR-CD3 BiTEs triggered an increase in expression levels of classic Treg markers FoxP3 and CD25 on activated Tregs (FoxP3^{++}CD45RA$^-$) and resting Tregs (FoxP3$^+$CD45RA$^+$; **Fig. 1G**; Supplementary Fig. S3B, Treg gating strategy).

EGFR-Vδ2 bsTCEs trigger Vγ9Vδ2 T-cell activation and cytotoxicity using healthy donor PBMCs

To assess whether EGFR-Vδ2 bsTCEs could mediate tumor cell lysis using PBMCs instead of expanded Vγ9Vδ2 T cells, healthy donor PBMCs [$n = 12$, Vγ9Vδ2 T-cell frequency: 0.05%–9.0% (range) of total T cells] were cultured for 7 days with SW480 tumor cells. Although some tumor lysis was observed in the control condition, likely due to alloreactivity, this was significantly enhanced in the presence of EGFR-Vδ2 bsTCEs and depended on the presence of Vγ9Vδ2-T cells, as no antitumor effect was observed when these were depleted from PBMCs (Supplementary Fig. S4A). Baseline PBMC Vγ9Vδ2 T-cell frequency did not correlate with the extent of tumor lysis (Supplementary Fig. S4B), which could (in the absence of consistent Vγ9Vδ2 T-cell expansion) point toward the involvement of other immune cells after the initial activation of Vγ9Vδ2 T cells. In cultures containing EGFR-Vδ2 bsTCEs, we not only observed strong Vγ9Vδ2 T-cell activation but also increased CD25 expression on CD4$^+$ and CD8$^+$ T cells and NK cells (CD56^{dim}CD16$^+$ and CD56$^+$CD16$^-$ cells; Supplementary Fig. S4C). The EGFR-Vδ2 bsTCE–induced CD25 upregulation on T and NK cells was significantly reduced or even abrogated in the presence of IFNγ-specific and TNF-specific neutralizing antibodies (Supplementary Fig. S4D), demonstrating this downstream activation to be at least in part cytokine driven. To explore whether activated T and NK cells contributed to the observed tumor lysis in SW480-PBMC cocultures, we evaluated the effect of HLA class I and II neutralizing antibodies and found that blocking HLA class I, but not class II, significantly reduced tumor lysis, suggesting the involvement of HLA class I–restricted CD8$^+$ T cells (Supplementary Fig. S4E). To further substantiate these findings, the impact of depletion of specific cell subsets from PBMCs (i.e., Vδ2$^+$, CD8α$^+$, CD8β$^+$, CD4$^+$, and CD56$^+$ cells) on EGFR-Vδ2 bsTCE–induced SW480 lysis was assessed. Although depletion of Vδ2$^+$ cells completely abrogated tumor lysis (Supplementary Fig. S4F), depletion of CD4$^+$, CD8β$^+$, and CD56$^+$ cells had limited to no impact. Depletion of CD8α$^+$ cells resulted in a trend toward reduced tumor lysis (range of frequency of CD8α$^+$ Vγ9Vδ2 T cells: 10%–33%). When comparing lysis of SW480 using whole PBMCs, EGFR-CD3 BiTEs were found to induce more lysis at lower concentrations than the EGFR-Vδ2 bsTCE (Supplementary Fig. S4G).

Cancer patient–derived Vγ9Vδ2 T cells display immune-checkpoint profiles that are distinct from that of conventional T cells

Vγ9Vδ2 T-cell frequency and phenotype were evaluated in healthy donors and patients with EGFR$^+$ cancers. The frequency of Vγ9Vδ2 T cells was comparable in healthy donor and cancer patient PBMCs (Supplementary Fig. S5A). However, a shift toward more effector-memory (CD27$^-$CD45RA$^-$) and terminally differentiated (CD27$^-$CD45RA$^+$) Vγ9Vδ2 T cells was evident in PBMCs from esophageal cancer patients (Supplementary Fig. S5B). Tumor samples from patients with primary and metastatic colorectal cancer and primary esophageal cancer contained 1.46% ± 1.44% Vγ9Vδ2 T cells among total T cells (Supplementary Fig. S5C). The Vγ9Vδ2 T-cell frequency did not significantly differ between malignant and (matched) nonmalignant tissue. Expression of immune-checkpoint receptors CTLA-4, PD-1, LAG-3, and TIM-3 was assessed on Vγ9Vδ2 T, CD4$^+$, and CD8$^+$ T cells in PBMCs of healthy donors and cancer patients with primary and metastatic colorectal cancer, primary esophageal cancer, and malignant and nonmalignant tissue samples of patients with primary and metastatic colorectal cancer. In PBMCs and tumor samples, a significantly higher percentage of CD4$^+$ and CD8$^+$ T cells expressed PD-1 as compared with Vγ9Vδ2 T cells, on which expression was low/absent (**Fig. 2**). CTLA-4 expression was low on Vγ9Vδ2 T cells in healthy donor PBMCs, but it was expressed at significantly higher levels on Vγ9Vδ2 T cells in cancer patient PBMCs. CTLA-4 levels were comparable between Vγ9Vδ2 T cells and CD4$^+$ and CD8$^+$ T cells in both PBMCs and tumor tissue. Expression of LAG-3 and TIM-3 was low on all subsets, but it tended to be lower on tumor-infiltrating Vγ9Vδ2 T cells (Supplementary Fig. S5D and S5E).

EGFR-Vδ2 bsTCEs trigger activation and cytotoxic activity of Vγ9Vδ2 T cells in cancer patient PBMCs and colorectal cancer samples

Tumor lysis triggered by EGFR-Vδ2 bsTCEs was also tested in 7-day cocultures of SW480 tumor cells and PBMCs from patients with primary colorectal cancer and primary esophageal cancer.

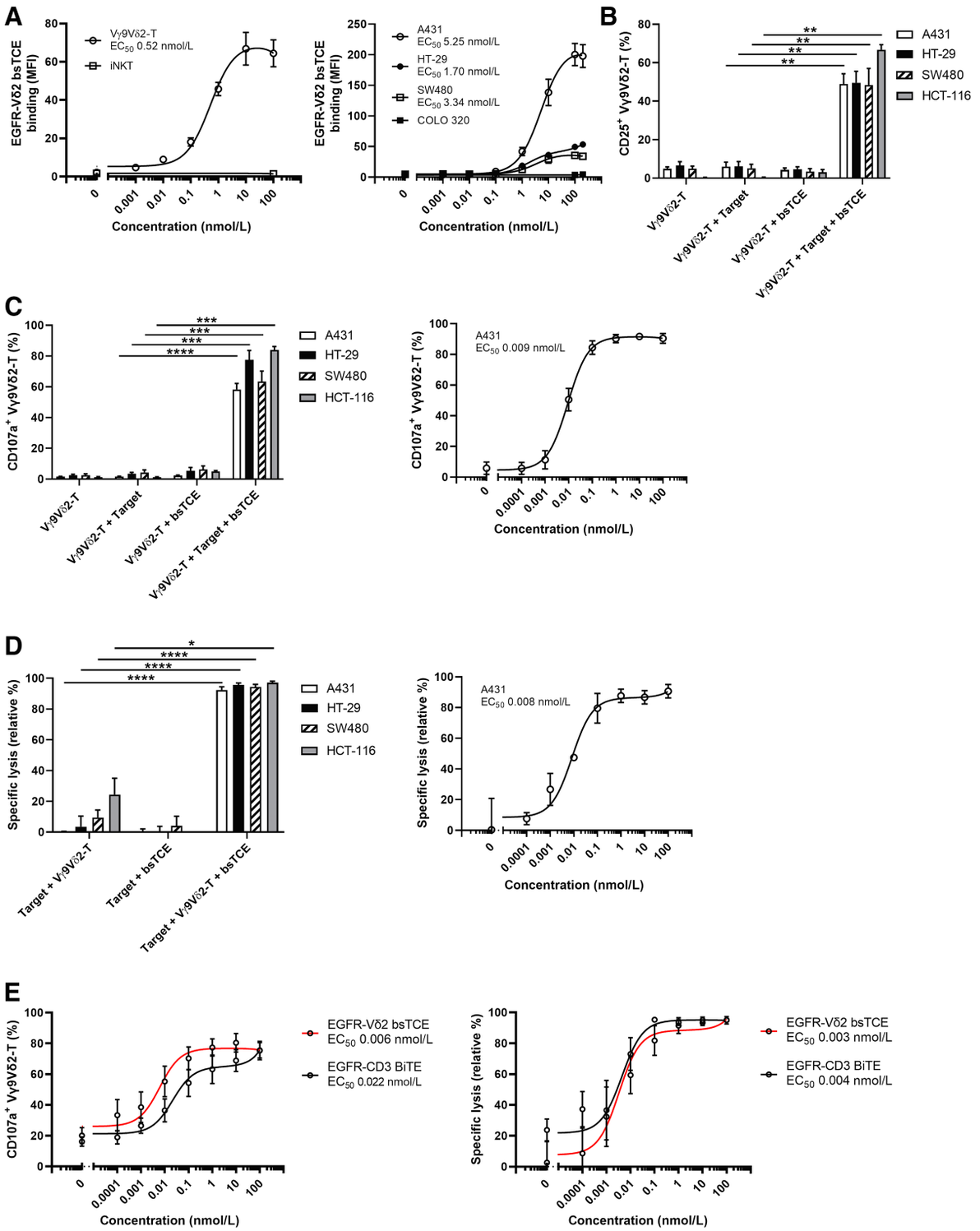

Figure 1.

EGFR-Vδ2 bsTCEs activate Vγ9Vδ2 T cells to lyse EGFR$^+$ tumor cells and EGFR-CD3 BiTEs induce Treg activation and effector T-cell suppression. **A,** Mean fluorescence intensity (MFI) of binding of EGFR-Vδ2 bsTCE to Vγ9Vδ2 T cells or iNKT cells and A431, HT-29, SW480, or COLO320 tumor cells ($n = 3$ per cell type) as assessed by flow cytometry. Expression of CD25 (**B**; $n = 5$ Vγ9Vδ2 T-cell donors) after 24 hours and CD107a (**C**; $n = 3$ Vγ9Vδ2 T-cell donors) after 4 hours on Vγ9Vδ2 T cells cocultured with A431, HT-29, SW480, or HCT-116 (1:1 E:T ratio; ± 50 nmol/L or concentration range of EGFR-Vδ2 bsTCE) as assessed by flow cytometry. **D,** Specific lysis (relative to tumor alone condition) of A431, SW480, HT-29, or HCT-116 after 24-hour incubation with Vγ9Vδ2 T cells (1:1 E:T ratio) ± 50 nmol/L or concentration range of EGFR-Vδ2 bsTCE ($n = 4$ Vγ9Vδ2 T-cell donors) as assessed by flow cytometry. **E,** Vγ9Vδ2-T cell CD107a expression ($n = 5$ Vγ9Vδ2-T cell donors, 4 hours) and SW480 cytotoxicity ($n = 4$ Vγ9Vδ2-T cell donors, 24 hours) following coculture of Vγ9Vδ2 T cells and SW480 tumor cells (1:1 E:T ratio) ± concentration range of EGFR-Vδ2 bsTCE or EGFR-CD3 BiTE as assessed by flow cytometry. (*Continued on the following page.*)

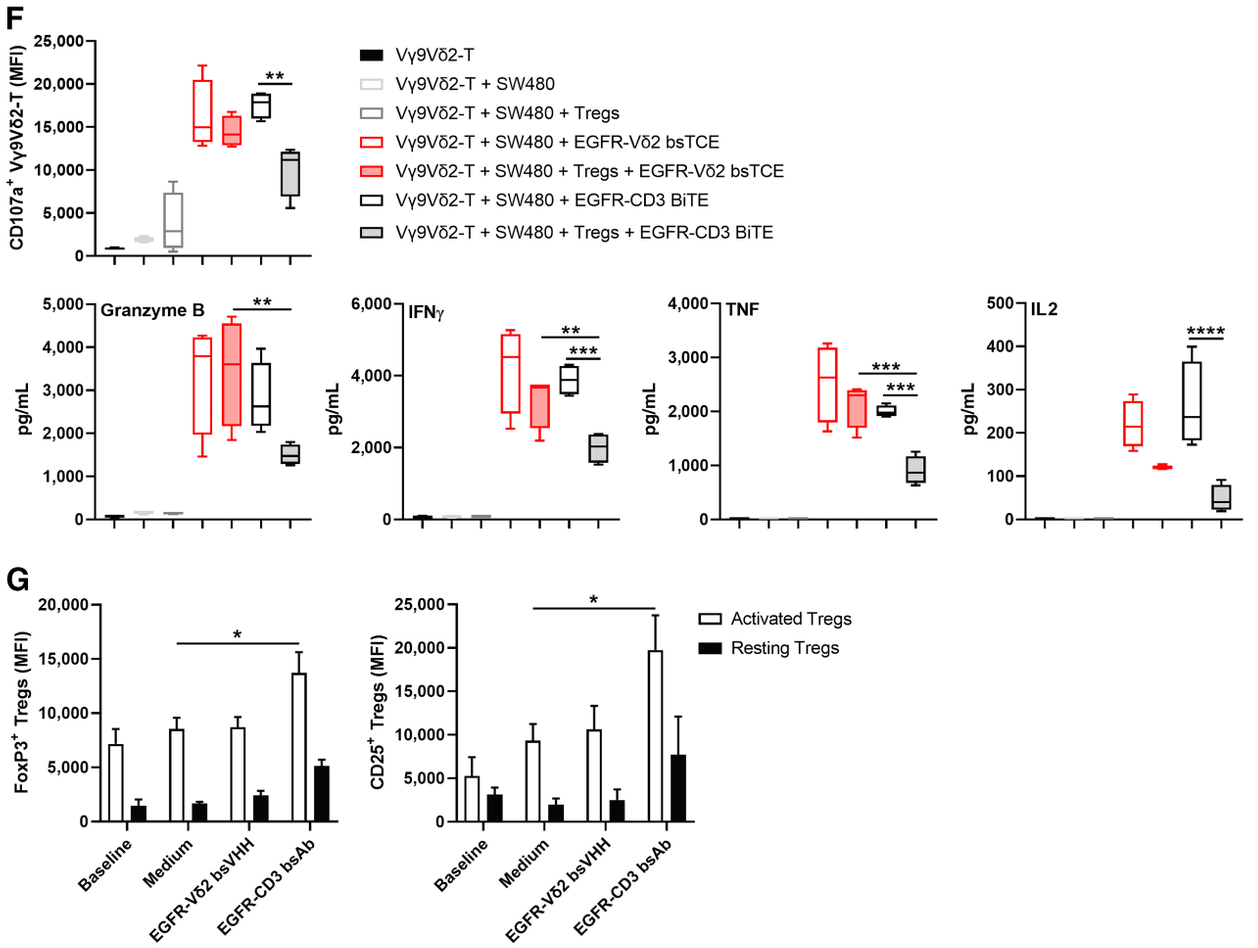

Figure 1.

(*Continued.*) **F,** Vγ9Vδ2 T-cell CD107a expression, as assessed by flow cytometry, and levels of granzyme-B, IFNγ, TNF, and IL2, as assessed by CBA, in 24-hour supernatants of cocultures of Vγ9Vδ2 T cells ($n = 3$), healthy donor–derived Tregs ($n = 4$), and SW480 tumor cells ± 50 nmol/L EGFR-Vδ2 bsTCE or EGFR-CD3 BiTEs. **G,** Flow-cytometric analysis of FoxP3 and CD25 expression on activated ($n = 8$) and resting ($n = 2$) Tregs in single-cell suspensions derived from colorectal cancer peritoneal metastases before (baseline) and after a 48-hour incubation ± 50 nmol/L EGFR-Vδ2 bsTCE or EGFR-CD3 BiTE. Data represent mean and SEM (**A–D, E, G**) and box and whisker plots indicate the median, 25th to 75th percentiles and minimum to maximum (**F**). *, $P < 0.05$, **, $P < 0.01$, ***, $P < 0.001$, ****, $P < 0.0001$. Paired *t* test (**B–D, G**), One-way ANOVA with Dunnet multiple comparisons test (**F**).

Although cancer patient PBMCs alone lysed SW480 cells, likely due to alloreactivity, the addition of EGFR-Vδ2 bsTCEs significantly enhanced cytolytic activity (Supplementary Fig. S6). To avoid alloreactivity, lytic activity was also assessed in 7-day cocultures of metastatic colorectal cancer patient–derived tumor cells and autologous PBMCs. EGFR-Vδ2 bsTCEs triggered substantial tumor lysis (**Fig. 3A**) and the secondary activation of T and NK cells was also confirmed in this setting (**Fig. 3B**).

We next evaluated whether EGFR-Vδ2 bsTCEs could activate Vγ9Vδ2 T cells present in the immunosuppressed tumor microenvironment. Even in 4-hour cultures of single-cell suspensions of primary and metastatic colorectal cancer samples, EGFR-Vδ2 bsTCEs triggered significant degranulation of tumor-infiltrated Vγ9Vδ2 T cells (**Fig. 3C**). Moreover, when tumor-infiltrated T cells, isolated from primary or metastatic colorectal cancer patient samples, were cocultured with autologous patient-derived colorectal cancer cells, the addition of EGFR-Vδ2 bsTCEs resulted in substantial tumor lysis (**Fig. 3D**).

Selective tumor cell killing by EGFR-Vδ2 bsTCE–activated Vγ9Vδ2 T cells

CD3 bsTCEs can induce on-target, off-tumor toxicity due to shared target-antigen expression on healthy cells, thereby redirecting T cells toward normal tissues, causing damage (31). Because EGFR is not exclusively expressed on tumor tissue (32, 33), Vγ9Vδ2 T-cell redirection and reactivity to normal EGFR-expressing tissue by the EGFR-Vδ2 bsTCE was tested. For this purpose, single-cell suspensions of EGFR-expressing nonmalignant colon, peritoneum, and liver tissue (derived from colorectal cancer patients) were cultured ± EGFR-Vδ2 bsTCE. The EGFR-Vδ2 bsTCEs did not increase degranulation of tissue-infiltrated Vγ9Vδ2 T cells in nonmalignant colon and peritoneum cultures, but a moderate increase in Vγ9Vδ2 T-cell degranulation was observed using nonmalignant liver tissue (**Fig. 4A**). Next, EGFR-Vδ2 bsTCE–induced cytotoxicity mediated by Vγ9Vδ2 T cells toward malignant and nonmalignant cells was compared by incubating expanded healthy donor–derived Vγ9Vδ2 T cells with single-cell suspensions of various malignant tumors (i.e., primary and metastatic

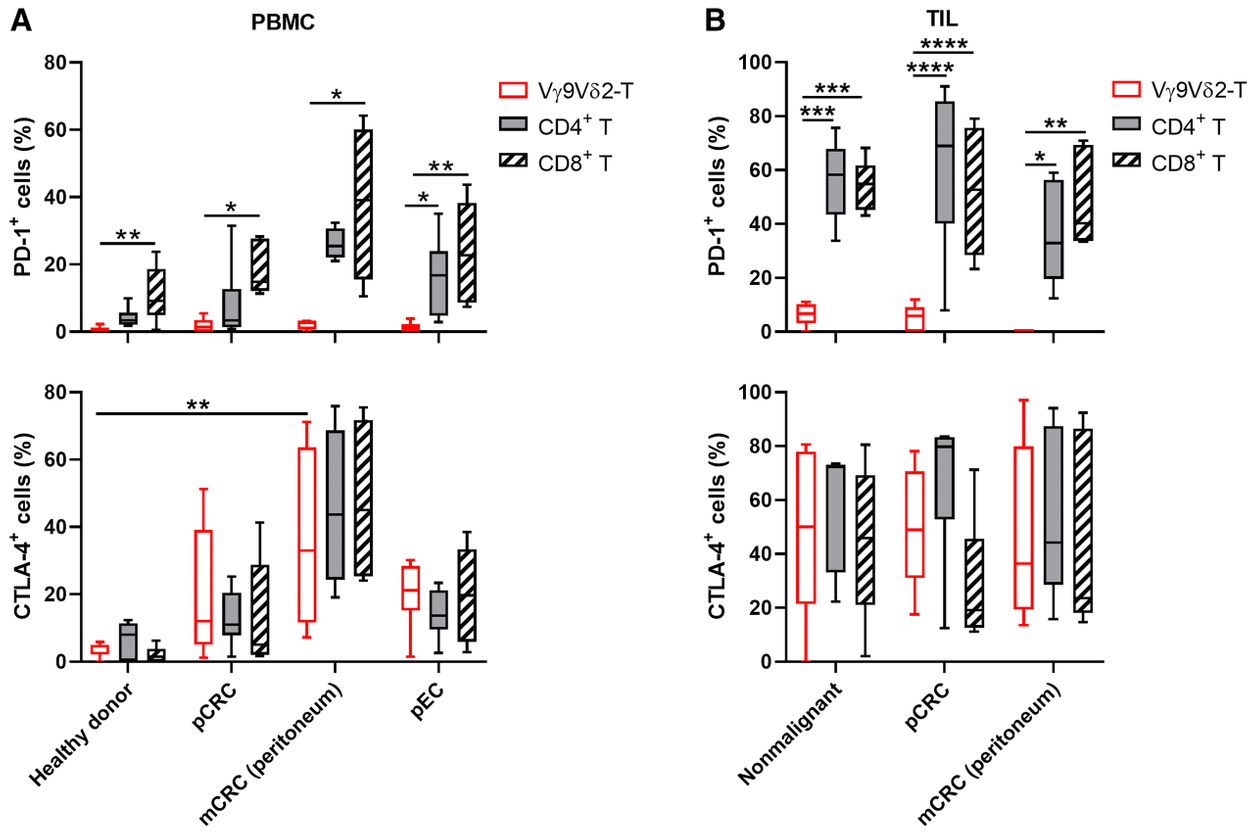

Figure 2.

Cancer patient Vγ9Vδ2 T cells have a distinct inhibitory immune-checkpoint receptor expression pattern. **A,** Flow-cytometric analysis of PD-1 and CTLA-4 expression on PB Vγ9Vδ2 T cells, $CD4^+$ T cells, and $CD8^+$ T cells derived from healthy donors ($n = 7$) and cancer patients with primary colorectal cancer ($n = 6$), peritoneal colorectal cancer metastases ($n = 4$), or primary esophageal cancer ($n = 8$). **B,** PD-1 and CTLA-4 expression on Vγ9Vδ2 T cells, $CD4^+$ T cells and $CD8^+$ T cells in dissociated nonmalignant tissue (colon tissue: $n = 2$ and peritoneum tissue: $n = 3$) and tumor tissue (primary colorectal cancer: $n = 8$ and peritoneal colorectal cancer metastases: $n = 5$) derived from cancer patients, as assessed by flow cytometry. Box and whisker plots indicate the median, 25th to 75th percentiles and minimum to maximum. *, $P < 0.05$; **, $P < 0.01$; ***, $P = <0.001$; ****, $P < 0.0001$. One-way ANOVA with Dunnet multiple comparisons test (**A, B**). TIL, tumor-infiltrating lymphocyte.

(liver, peritoneum) colorectal cancer, head and neck squamous cell carcinoma, and non–small cell lung carcinoma) and paired nonmalignant tissue (colon, peritoneum, and liver). Although EGFR-Vδ2 bsTCEs induced Vγ9Vδ2 T cells to substantially lyse patient-derived tumor cells, no lysis of paired nonmalignant tissues by Vγ9Vδ2 T cells was observed (**Fig. 4B**). Primary and metastatic colorectal cancer and esophageal cancer samples typically expressed higher levels of EGFR as well as BTN3A, with which Vγ9Vδ2 T cells naturally interact, compared with nonmalignant colon (mean MFI EGFR: 6.4 vs. 0.8 and BTN3A: 44.1 vs. 8.2), peritoneal (mean MFI EGFR: 23.3 vs. 14.1 and BTN3A: 110.6 vs. 55.7), liver (mean MFI EGFR: 19.3 vs. 4.8 and BTN3A: 108.0 vs. 63.4), and esophageal tissue (mean MFI EGFR: 15.0 vs. 2.3 and BTN3A: 72.1 vs. 16.7; **Fig. 4C**). EGFR and BTN3A expression was consistently higher on malignant compared with nonmalignant cells of the same individual patient, and expression was also higher on metastatic compared with primary colorectal cancer. We next assessed the relative contribution of tumor cell–expressed EGFR and BTN3A and the Vγ9Vδ2 T-cell costimulatory receptor NKG2D, expressed by expanded healthy donor Vγ9Vδ2 T cells (Supplementary Fig. S7A), to EGFR-Vδ2 bsTCE–induced Vγ9Vδ2 T-cell activation. In both cocultures of the EGFR, BTN3A, and NKG2D ligand (MIC-A/B, ULPB-1, ULBP-3, ULBP-2/5/6)–expressing human colorectal cancer cell line WiDr (Supplementary Fig. S7B) and expanded Vγ9Vδ2 T cells as well as cocultures of metastatic colorectal cancer patient–derived tumor cells and autologous PBMCs, the EGFR-Vδ2 bsTCE–induced increase in Vγ9Vδ2 T-cell degranulation was reduced by EGFR-specific and/or NKG2D-specific blocking antibodies but was not significantly affected by blocking BTN3A (**Fig. 4D**). EGFR-Vδ2 bsTCE–induced Vγ9Vδ2 T-cell activation was most profoundly abrogated when interactions with EGFR, BTN3A, and NKG2D ligands were simultaneously blocked.

EGFR-Vδ2 bsTCEs trigger *in vivo* antitumor activity in mice inoculated with $EGFR^+$ RAS^{mt} and RAS^{wt} tumor cells and human PBMCs

We assessed the *in vivo* antitumor activity of EGFR-Vδ2 bsTCEs in NPG mice s.c. inoculated with 5×10^6 KRAS-mutant HCT-116 tumor cells alone or admixed with 5×10^6 PBMCs [$n = 2$ healthy human donors (10.7% and 4.8% Vγ9Vδ2-T of total T cells), $n = 4$ mice/PBMC donor/group] and treated with daily i.v. administration of PBS or EGFR-Vδ2 bsTCEs for 14 days. PBMC (containing a nonenriched and nonpreactivated population of Vγ9Vδ2 T cells) were used as effector cells instead of expanded purified Vγ9Vδ2 T cells as we reasoned this would be more reflective of the effector cell population encountered in a future human clinical trial. Compared with the PBMC control group, treatment with 0.5 mg/kg or 5.0 mg/kg EGFR-Vδ2 bsTCE led

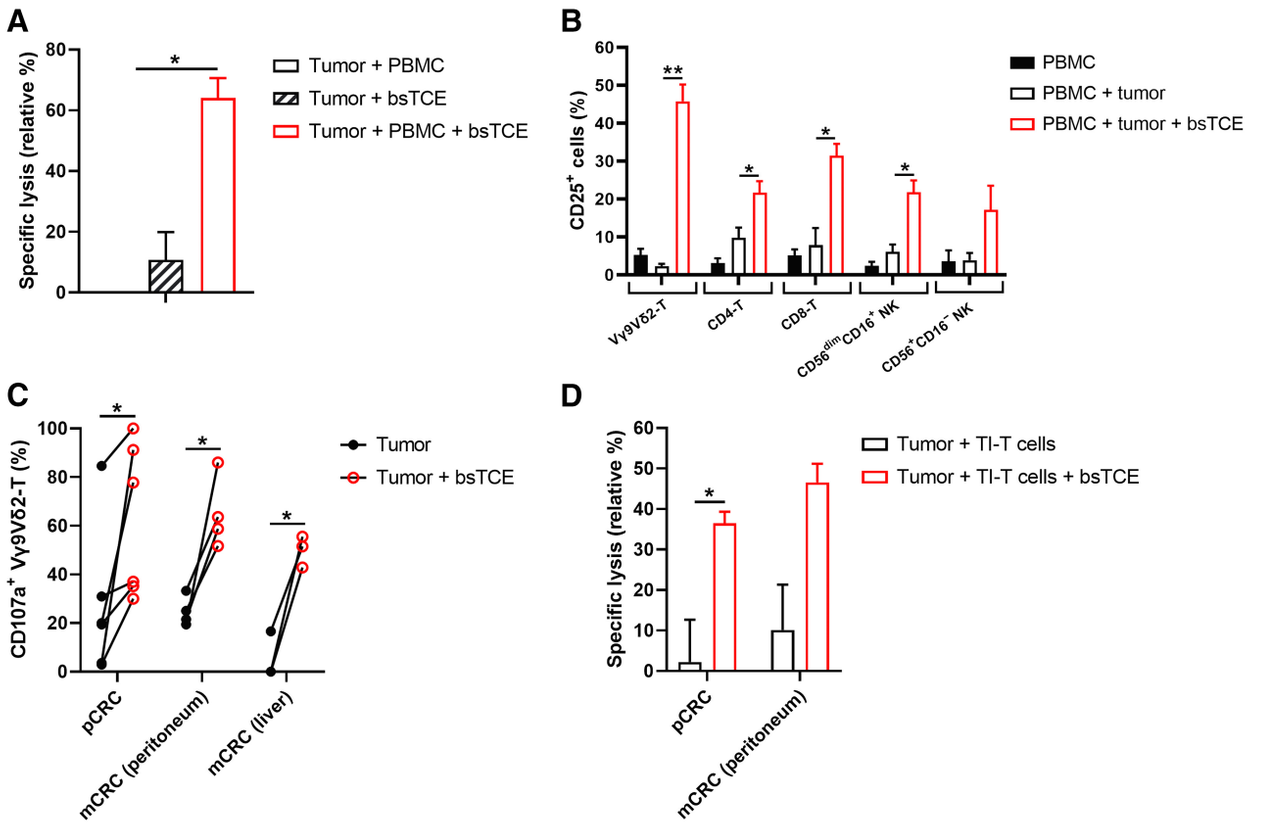

Figure 3.

PB and tumor-infiltrating Vγ9Vδ2 T cells of cancer patients can be activated by the EGFR-Vδ2 bsTCE to trigger autologous tumor cell lysis. **A,** Specific lysis of tumor cells (relative to tumor alone condition) after a 7-day coculture of dissociated tumor cells (peritoneal metastases of colorectal cancer: $n = 3$) with autologous PBMCs (5:1 E:T ratio) and ± 50 nmol/L EGFR-Vδ2 bsTCE. **B,** CD25 expression on lymphocyte subsets after a 7-day culture of patient-dissociated peritoneal colorectal cancer metastases and autologous PBMC (5:1 E:T ratio, $n = 5$) ± 50 nmol/L EGFR-Vδ2 bsTCE. **C,** CD107a expression on tumor-infiltrating Vγ9Vδ2 T cells (primary colorectal cancer: $n = 6$, peritoneal colorectal cancer metastases: $n = 4$ and liver colorectal cancer metastases: $n = 3$) after a 4-hour incubation ± 50 nmol/L EGFR-Vδ2 bsTCE. **D,** Specific lysis (relative to tumor alone condition) of tumor cells after a 24-hour culture of patient-dissociated tumor cell suspensions (primary colorectal cancer: $n = 4$ and peritoneal colorectal cancer metastases: $n = 3$) with autologous tumor-infiltrating total T-cell fractions (TI-T cells, 1:1 E:T ratio) ± 50 nmol/L EGFR-Vδ2 bsTCE. Data are all generated through flow cytometry and represent mean and SEM *, $P < 0.05$; **, $P < 0.01$. Paired *t* test (**A–D**).

to significant tumor growth inhibition resulting in increased overall survival (median OS/group: PBS and PBMC 28 days, 0.5 mg/kg bsTCE 48 days and 5.0 mg/kg bsTCE 42 days; **Fig. 5A**). No statistically significant difference was found between mice receiving 0.5 or 5.0 mg/kg EGFR-Vδ2 bsTCE. **Figure 5B** shows individual tumor growth curves. One mouse in the 5.0 mg/kg EGFR-Vδ2 bsTCE group had no palpable tumor at the end of the experiment. Antitumor activity was also assessed using a half-life extended EGFR-Vδ2-Fc bsTCE. NPG mice were s.c. inoculated with 5×10^6 A431 tumor cells admixed with 5×10^6 PBMCs [$n = 1$ healthy human donor (8.4% Vγ9Vδ2-T of total T cells), $n = 8$ mice/group] and treated with weekly i.v. administration of PBS or EGFR-Vδ2-Fc bsTCE (2 mg/kg) until termination of the experiment on day 21. As illustrated in **Fig. 5C** and **D**, treatment with EGFR-Vδ2-Fc bsTCE resulted in a significantly lower tumor volume (tumor growth inhibition 27.7% ± 6.3%; mean ± SEM).

BsTCE targeting of Vγ9Vδ2 T cells to EGFR shows no signs of toxicity, including CRS, despite evidence of target engagement in *macaca fascicularis*

Although little *in vitro* reactivity of Vγ9Vδ2 T cells toward normal EGFR$^+$ cells was observed after treatment with the EGFR-specific Vγ9Vδ2 T cell–activating bsTCE, the widespread expression of EGFR in normal tissues could pose a concern for clinical testing of the approach. Therefore, the safety of targeting Vγ9Vδ2 T cells to EGFR was explored in female NHP *Macaca fascicularis* (cynomolgus monkey). As the Vδ2 TCR–specific VHH lacked cross-reactivity to the NHP Vγ9Vδ2 TCR (34) and there are, to the best of our knowledge, no known Vδ2 TCR–specific NHP cross-reactive mAbs, surrogate engagers were generated where EGFR-specific VHH-7D12 was fused to a cross-reactive scFv derived from anti-Vγ9 mAb clone 7A5 (27). In cocultures of human Vγ9Vδ2 T cells and EGFR$^+$ tumor cells, EGFR-Vγ9 bsTCE and EGFR-Vδ2 bsTCE induced comparable (low pM EC_{50}) Vγ9Vδ2 T-cell degranulation and tumor lysis (Supplementary Fig. S8A). EGFR-Vγ9 bsTCE binding to cynomolgus Vγ9$^+$ T cells and recombinant cynomolgus EGFR was confirmed (Supplementary Fig. S8B) and EGFR-Vγ9 bsTCE triggered NHP Vγ9Vδ2 T-cell degranulation in 24-hour cultures with plate-bound recombinant cynomolgus EGFR (Supplementary Fig. S8C). In a first NHP study, a single dose or 7 daily doses (0.03 mg/kg, 0.1 mg/kg, or 0.3 mg/kg) of EGFR-Vγ9 bsTCE were infused (30 minutes, i.v., $n = 1$/dose). Neither single nor multiple doses resulted in clinical signs of toxicity, and no relevant changes in clinical chemistry, hematology, or coagulation

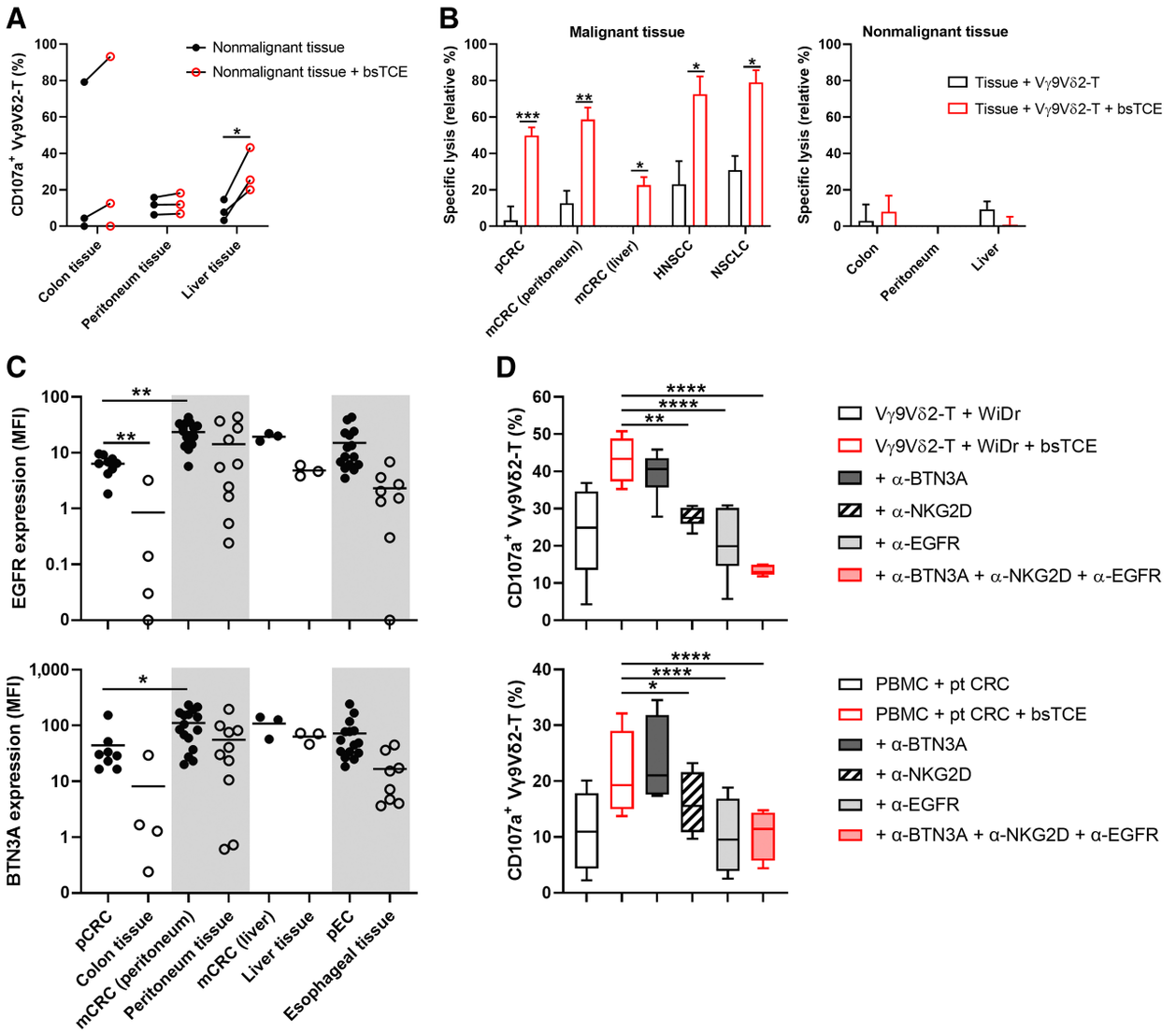

Figure 4.

EGFR-Vδ2 bsTCE–activated Vγ9Vδ2 T cells exert tumor preferential activity. **A,** CD107a expression on Vγ9Vδ2 T cells present in nonmalignant colon ($n = 3$), peritoneum ($n = 3$), and liver tissue ($n = 3$) after a 4-hour incubation ± 50 nmol/L EGFR-Vδ2 bsTCE. **B,** Specific lysis (relative to tissue alone condition) of malignant and nonmalignant cells after a 4-hour culture of dissociated tumor cell suspensions (primary colorectal cancer, $n = 10$; peritoneal colorectal cancer metastases, $n = 5$; liver colorectal cancer metastases, $n = 3$; primary HNSCC, $n = 5$; and primary NSCLC, $n = 4$) or dissociated nonmalignant cell suspensions (colon tissue, $n = 3$; peritoneum tissue, $n = 4$; and liver tissue, $n = 3$) with healthy donor–derived Vγ9Vδ2 T cells (1:1 E:T ratio) ± 50 nmol/L EGFR-Vδ2 bsTCE. **C,** Expression of EGFR and BTN3A on dissociated tumor [primary colorectal cancer, $n = 9$ (EGFR) and $n = 8$ (BTN3A); peritoneal colorectal cancer metastases; $n = 16$; liver colorectal cancer metastases, $n = 3$; and primary esophageal cancer, $n = 15$] and nonmalignant tissue (colon, $n = 4$; peritoneum, $n = 10$; liver, $n = 3$; and esophageal, $n = 8$) derived from cancer patients. **D,** CD107a expression on expanded Vγ9Vδ2 T cells ($n = 6$) after a 4-hour coculture with WiDr tumor cells (1:1 E:T ratio) or Vγ9Vδ2 T cells in PBMCs of patients with peritoneal colorectal cancer metastases ($n = 4$) after a 4-hour coculture with matched autologous tumor cells suspensions (5:1 E:T ratio). Where indicated, Vγ9Vδ2 T cells were preincubated with 10 μg/mL anti-Fc receptor and/or NKG2D-specific blocking Ab, and tumor cells were preincubated ± 10 μg/mL BTN3A-specific blocking Ab or EGFR-specific blocking Ab ± 10 pmol/L EGFR-Vδ2 bsTCE. Data are all generated through flow cytometry and represent mean and SEM (**B**), mean (**C**) and box and whisker plots indicate the median, 25th to 75th percentiles and minimum to maximum (**D**). *, $P < 0.05$; **, $P < 0.01$; ***, $P < 0.001$; ****, $P < 0.0001$. Paired *t* test (**A, B**) and one-way ANOVA with Dunnet multiple comparisons test (**C, D**).

tests were observed in the animals that received multiple doses (Supplementary Table S5). Necropsy showed no gross macroscopic nor histopathologic abnormalities. EGFR-Vγ9 bsTCE plasma concentrations could be detected for up to 8 hours (0.1 mg/kg) and 48 hours (0.03 mg/kg, half-life 13.7 hours; 0.3 mg/kg, half-life 7.9 hours; **Fig. 6A**). In animals receiving multiple doses, cytokine levels were assessed. Although there were no changes in the levels of IL1β (all < 0.9 pg/mL), IL2 (all < 7.7 pg/mL), IL4 (all < 0.9 pg/mL), IL5 (all < 4.8 pg/mL), IL8 (all < 2.9 pg/mL), IL10 (all < 2.1 pg/mL), TNF (all < 2.7 pg/mL), IFNγ (all < 13.9 pg/mL), and IL12p70

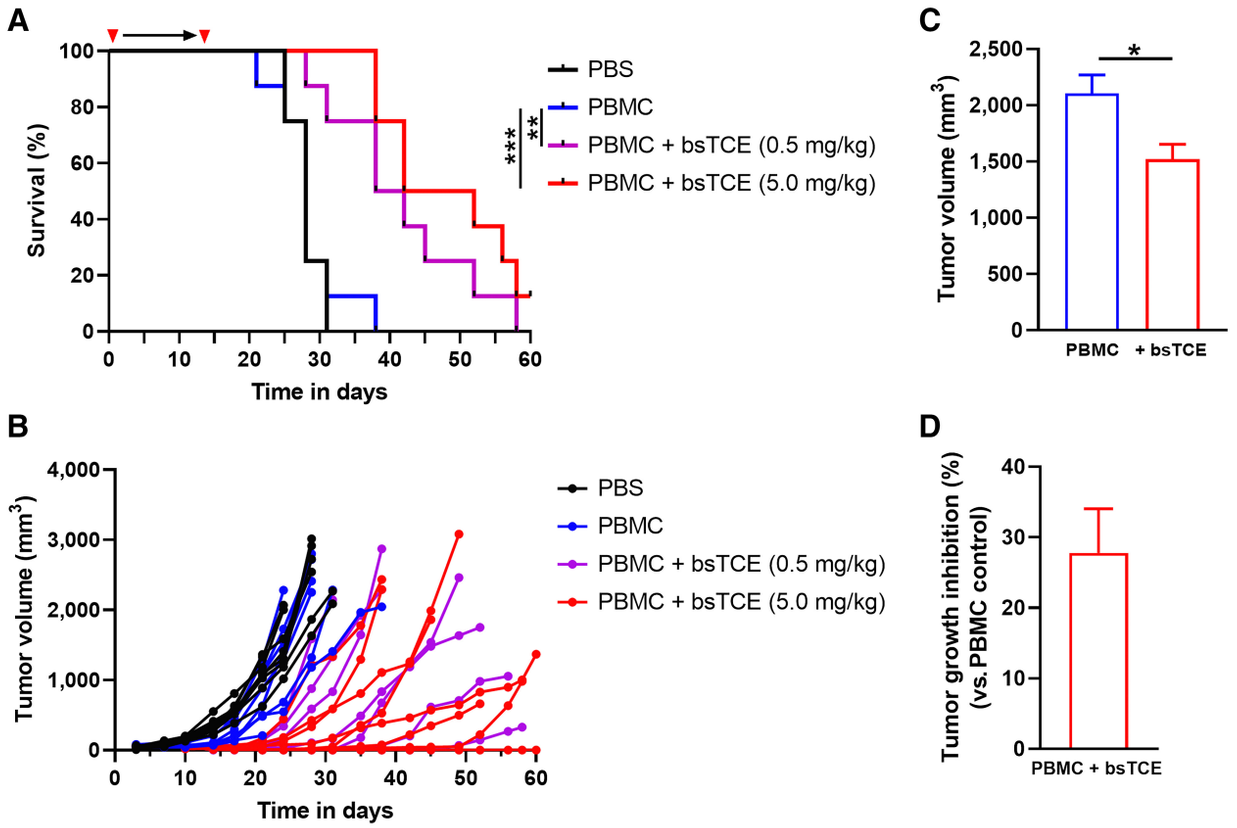

Figure 5.

EGFR-Vδ2 bsTCE has antitumor activity in immunodeficient NPG mice in combination with PBMCs. NPG mice were engrafted s.c. with HCT-116 tumor cells alone or admixed with PBMCs and treated with PBS (control groups), 0.5 mg/kg or 5.0 mg/kg EGFR-Vδ2 bsTCE ($n = 8$ mice per group, $n = 4$ mice per PBMC donor). EGFR-Vδ2 bsTCE was administered daily for 14 days. Overall survival of mice (**A**) and tumor volume in mm^3 (**B**) were measured over the course of 60 days (individual curves are shown). NPG mice were engrafted s.c. with A431 tumor cells admixed with PBMCs and treated weekly with PBS (control group) or 2.0 mg/kg EGFR-Vδ2-Fc bsTCE ($n = 8$ mice per group) until study termination at day 21. Day 21 tumor volume (**C**; mean ± SEM) and percent EGFR-Vδ2-Fc bsTCE–mediated tumor growth inhibition (**D**; mean ± SEM). *, $P < 0.05$; **, $P < 0.01$; ***, $P < 0.001$. Mantel–Cox test (**A**), unpaired t test (**C**). Red arrowheads indicate EGFR-Vδ2 bsTCE infusion.

(all < 12.6 pg/mL), a mild increase in IL6, IL15, and MCP-1 was observed in the first 24 hours after the first administration of the highest EGFR-Vγ9 bsTCE dose (**Fig. 6B**).

Various leukocyte populations were monitored in PB, including neutrophilic granulocytes, monocytes, B cells, CD4$^+$ and CD8$^+$ T cells, and NK cells. Apart from changes typically observed in response to i.v. drug administrations in NHP studies (e.g., temporary increase in neutrophilic granulocytes, temporary decrease in monocyte and lymphocyte counts), no significant persistent changes were observed. Kinetics of PB T-cell numbers are shown in Supplementary Fig. S9A and S9B. Vγ9$^+$ T cells were studied more extensively. After a single EGFR-Vγ9 bsTCE dose, a rapid drop in Vγ9$^+$ T-cell counts was noted regardless of the administered dose (**Fig. 6C**), although these counts recovered to approximate baseline within 1 to 3 days. In NHPs receiving multiple doses, a similar rapid drop and subsequent recovery of PB Vγ9$^+$ T-cell numbers was observed (Supplementary Fig. S9C). EGFR-Vγ9 bsTCE binding to PB Vγ9$^+$ T cells was observed at all dose levels in both single- and multiple-dosed animals. After a single administration, EGFR-Vγ9 bsTCE binding intensity to Vγ9$^+$ T cells gradually decreased becoming (flow-cytometrically) undetectable after ∼3 days (**Fig. 6D**). With daily dosing, EGFR-Vγ9 bsTCE binding to PB Vγ9$^+$ T cells was observed more consistently over time (**Fig. 6E**) and EGFR-Vγ9 bsTCE binding to lymph node Vγ9$^+$ T cells was detectable in the animal treated with the highest dose (Supplementary Fig. S9D). Indicative of bispecific engagement, an early and temporary increase in expression of activation markers CD25 and CD69 was observed on PB Vγ9$^+$ T cells after dosing (**Fig. 6F**) and on lymph node Vγ9$^+$ T cells in the animal treated with multiple doses at the highest dose level (Supplementary Fig. S9E).

We next assessed the safety, pharmacokinetics, and pharmacodynamics of a half-life extended (inert Fc containing) EGFR-Vγ9 bsTCE. Binding of this bsTCE to cynomolgus Vγ9Vδ2-TCR and EGFR was confirmed (Supplementary Fig. S9F). The EC_{50} for Vγ9Vδ2 T-cell degranulation of the EGFR-Vγ9-Fc bsTCE (in the presence of A431 tumor cells) was slightly higher than that of the EGFR-Vγ9 bsTCE (EC_{50} 0.05 nmol/L vs. 0.01 nmol/L; Supplementary Fig. S9G). Female NHP received 4 weekly doses (1 mg/kg, 5 mg/kg, or 23 mg/kg, $n = 1$/dose) via a 30-minute i.v. infusion. EGFR-Vγ9-Fc bsTCE plasma concentrations could be detected 103 to 127 hours after administration and systemic exposure increased dose proportionally. In the 1 mg/kg EGFR-Vγ9-Fc bsTCE–dosed NHP, more rapid clearance and lower peak-concentration levels were noted after the third dose, possibly due to drug-specific antibody development (**Fig. 6G**). No clinical signs of toxicity and no relevant changes in hematologic and

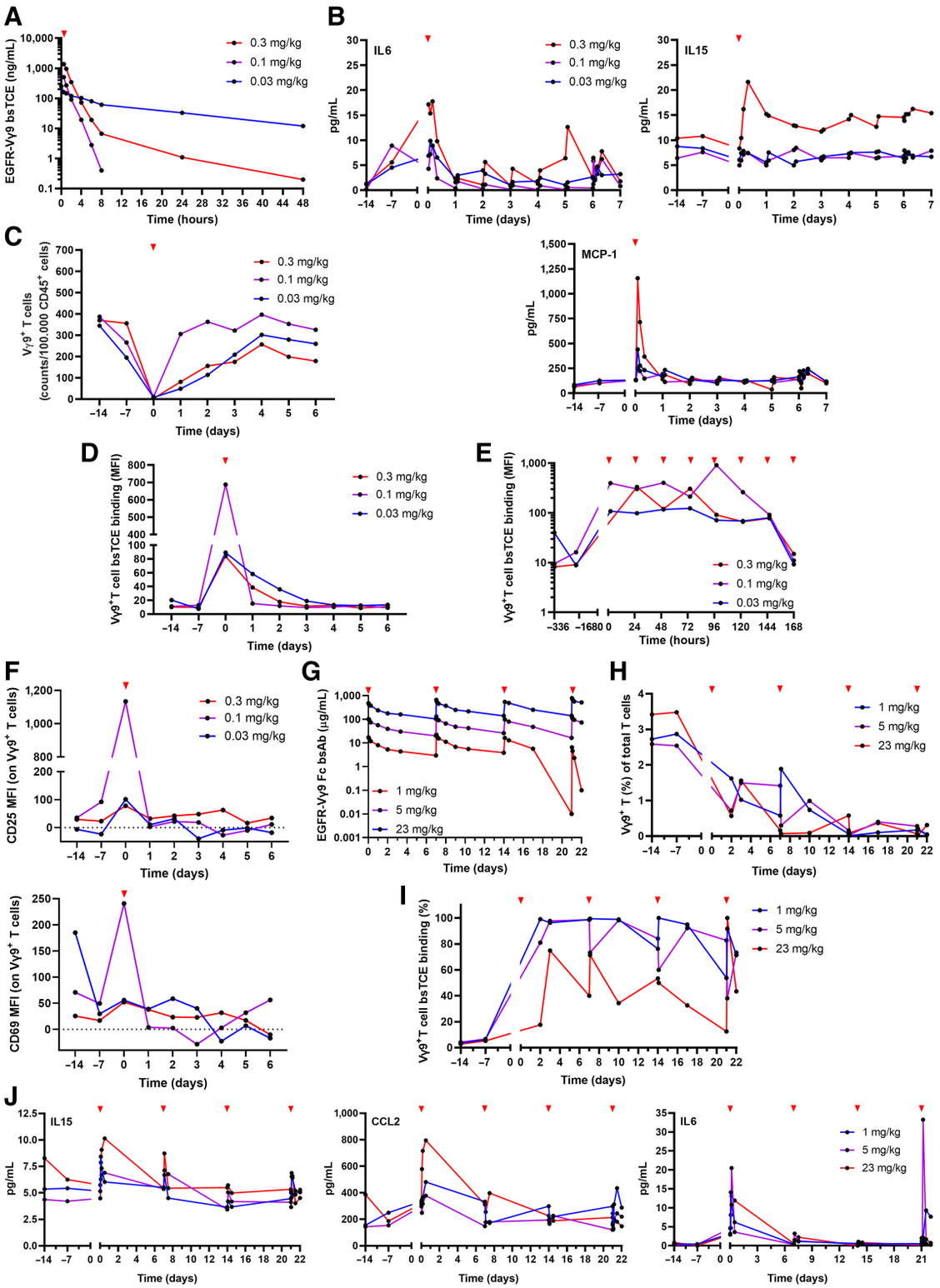

Figure 6.

Pharmacokinetic and pharmacodynamic effects of EGFR-Vγ9 bsTCE and EGFR-Vγ9-Fc bsTCEs in NHP. **A–F,** Single and multiple doses of the EGFR-Vγ9 bsTCE (0.03 mg/kg, 0.1 mg/kg, and 0.3 mg/kg, $n = 1$ per dose) were administered to female *Macaca fascicularis*. PB was collected to assess pharmacokinetics in the single-dose study (**A**), cytokines in the multiple-dose study (**B**), Vγ9$^+$ T-cell counts per 100,000 CD45$^+$ cells in the single-dose study (**C**), binding of EGFR-Vγ9 bsTCE to Vγ9$^+$ T cells in the single-dose study (**D**) and the multiple-dose study (**E**) and CD25 and CD69 expression on Vγ9$^+$ T cells in the single-dose study (**F**). (*Continued on the following page.*)

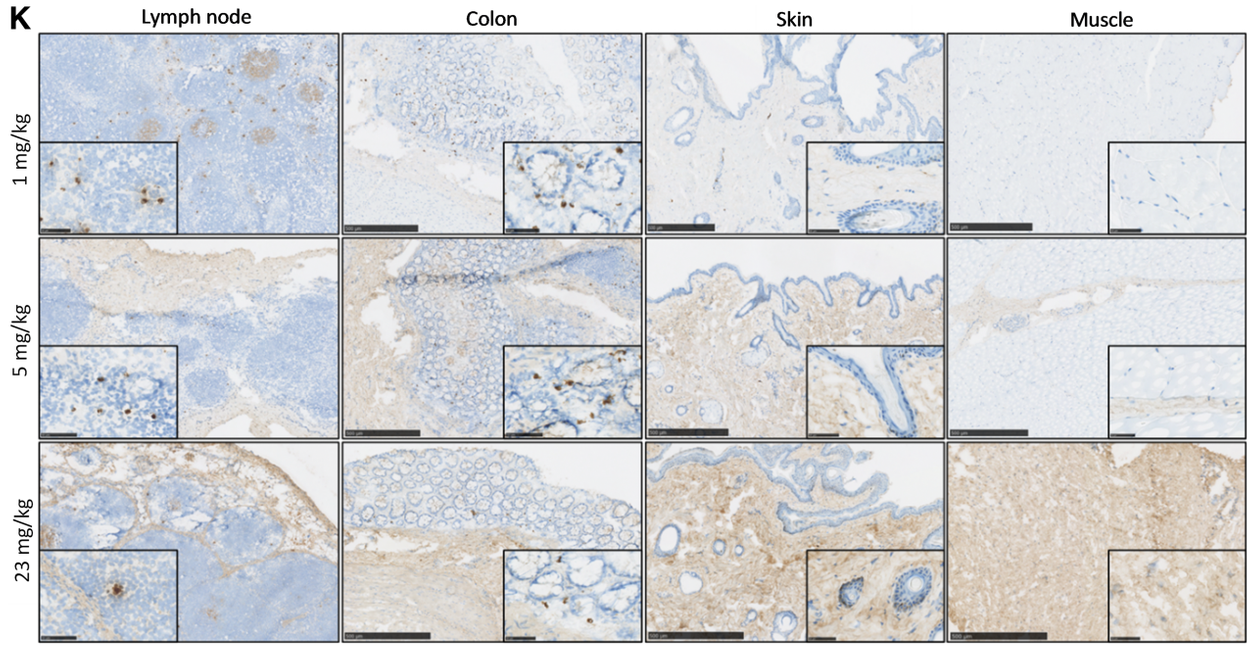

Figure 6.

(*Continued.*) **G–K,** Four weekly doses of EGFR-Vγ9-Fc bsTCE (1 mg/kg, 5 mg/kg, and 23 mg/kg, $n = 1$ per concentration) were administered to female *Macaca fascicularis*. PB was collected to assess pharmacokinetics (**G**), Vγ9$^+$ T (%) of total T cells (**H**), binding of EGFR-Vγ9-Fc bsTCE to Vγ9$^+$ T cells (**I**), both assessed through flow cytometry, and IL6, IL15, and CCL2 levels (**J**) assessed through ELISA. **K,** IHC detection of EGFR-Vγ9-Fc bsTCE on tissue slides derived from postmortem NHP lymph node, muscle, skin, and colon. EGFR-Vγ9-Fc bsTCE was visualized using HP-coupled anti-human IgG combined with Chomomap DAB (brown) and hematoxylin counterstain (blue). Scale bar, 500 μm, and a magnification is presented in the lower right corner with scale bar, 50 μm. Red arrowheads in **A–J** indicate EGFR-Vγ9 bsTCE or EGFR-Vγ9-Fc bsTCE infusion.

biochemical parameters were seen (Supplementary Table S6). Over time, PB Vγ9$^+$ T-cell frequencies declined (**Fig. 6H**), likely due to extravasation and retention in peripheral EGFR-expressing tissues, whereas EGFR-Vγ9-Fc bsTCE binding to Vγ9$^+$ T cells was maintained (**Fig. 6I**). Moderate increases in CD25 and CD69 expression on Vγ9$^+$ T cells, reflective of their activation, were observed (Supplementary Fig. S9H). Levels of IL1β (all < 0.1 pg/mL), IL2 (all < 8.7 pg/mL), IL4 (all < 0.1 pg/mL), IL5 (all < 1.4 pg/mL), IL8 (all < 2.0 pg/mL), IL10 (all < 1.0 pg/mL), TNF (all < 0.1 pg/mL), IFNγ (all < 0.2 pg/mL), and IL12p70 (all < 0.2 pg/mL) were measured in plasma, and mild EGFR-Vγ9-Fc bsTCE administration–related increases were observed for IL6, IL15, and MCP-1 (**Fig. 6J**) and typically most pronounced after the first administration. EGFR-Vγ9-Fc bsTCEs could be detected in NHP mesenteric lymph node, muscle, skin, and colon, and exposure increased with increasing doses administered (**Fig. 6K**), confirming that EGFR-Vγ9-Fc bsTCEs reached relevant tissue compartments. No compound-related microscopic findings were observed in tissues at necropsy (**Fig. 6K** shows representative data of lymph node, colon, skin, and muscle; a complete list of all tissues studied can be found in the Materials and Methods section).

Discussion

Vγ9Vδ2 T cells represent a unique proinflammatory effector T-cell population capable of lysing a large variety of tumors by sensing phosphoantigen-induced conformational alterations in tumor cell–expressed BTN2A1/BTN3A1 complexes (2, 3). Although the safety of Vγ9Vδ2 T cell–based therapeutic approaches was demonstrated in several clinical studies, antitumor efficacy has thus far been unsatisfactory (13, 35). Here, we report on the preclinical *in vitro*, *ex vivo*, and *in vivo* efficacy of a bispecific antibody designed to trigger conditional activation of Vγ9Vδ2 T cells against EGFR$^+$ tumor cells and demonstrated the safety of this approach in NHP using fully cross-reactive (surrogate) Vγ9Vδ2 T-cell engagers.

EGFR-Vδ2 bsTCEs triggered Vγ9Vδ2 T-cell activation, degranulation, and subsequent lysis of EGFR$^+$ tumor cells regardless of tumor KRAS/BRAF mutation status, and inhibited tumor growth and improved survival of mice inoculated with RAS^{mt} colorectal cancer cells and human PBMCs. Vγ9Vδ2 T-cell activation resulted in predominant production of proinflammatory cytokines such as IFNγ, TNF, and IL2. IL4 levels were only elevated in supernatants of Vγ9Vδ2 T cells cultured with A431 tumor cells, possibly due to IL4 release from lysed A431 (36). EGFR-Vδ2 bsTCEs also triggered increased levels of CCL5, CXCL10, and CXCL11 in cocultures of Vγ9Vδ2 T cells and EGFR$^+$ tumor cells, which could mediate activation, maturation, and chemotaxis of different immune cell subsets (37). Indeed, in cocultures of EGFR$^+$ tumor cell lines or patient-derived tumor cells and PBMCs, EGFR-Vδ2 bsTCEs facilitated IFNγ- and TNF-dependent downstream activation of CD4$^+$ and CD8$^+$ T cells and NK cells following Vγ9Vδ2 T-cell activation. Activated Vγ9Vδ2 T cells did not produce IL10 or IL17A, factors associated with suppressive/regulatory effects and tumor progression (38). EGFR-Vδ2 bsTCE–mediated control of tumor growth in cocultures of EGFR$^+$ tumor cells and PBMCs critically depended on the presence of Vγ9Vδ2 T cells and was additionally affected by blocking HLA class I interactions and depletion of CD8α$^+$ but not CD8β$^+$ cells. As depletion of CD8α$^+$ cells removes CD8αβ$^+$ T cells as well as CD8αα homodimer expressing NK, NKT, Vγ9Vδ2 T and other double-negative T-cell populations (39–42), some of which may be MHC-I–restricted, such populations may contribute to tumor control triggered by EGFR-Vδ2 bsTCE–activated Vγ9Vδ2 T cells.

Using PBMCs and esophageal cancer and primary- and metastatic colorectal cancer patient tumor samples, we confirmed Vγ9Vδ2 T-cell presence in both PB and tumors and showed Vγ9Vδ2 T cells to be skewed toward an effector-memory/terminally differentiated effector phenotype in cancer patients. In both PB and cancer patient tumors Vγ9Vδ2 T cells were also distinct from conventional $CD4^+$ and $CD8^+$ T cells in expressing lower LAG-3 and TIM-3 levels, and low to no PD-1, consistent with the absence of T-cell exhaustion (43). This profile suggests that Vγ9Vδ2 T cells, unlike conventional T cells, may be relatively resistant to immune checkpoint–mediated inhibition and position them as valid immune therapeutic targets, even under e.g., PD-1 blockade–resistant conditions. Although patient Vγ9Vδ2 T cells expressed variable levels of CTLA-4, ipilimumab mediated inhibition of CTLA-4 did not enhance EGFR-Vδ2 bsTCE–induced activation of $CTLA\text{-}4^+$ Vγ9Vδ2 T cells in cocultures with EGFR-expressing A431 tumor cells (percentage $CD69^+$ Vγ9Vδ2-T cells: baseline: 25.8% ± 0.9%, A431: 25.4% ± 10.3%, A431 + 0.1 nmol/L EGFR-Vδ2 bsTCE: 53.4% ± 1.5% and A431 + 0.1 nmol/L EGFR-Vδ2 bsTCE + 10 μg/mL ipilimumab: 47.6% ± 11.3%; $n = 3$, mean ± SD). Vγ9Vδ2 T cells present in primary- and metastatic colorectal cancer tissue degranulated within hours in the presence of EGFR-Vδ2 bsTCEs. Of particular interest was the observation that whereas EGFR-Vδ2 bsTCEs triggered Vγ9Vδ2 T cells to exert cytolytic activity against patient colorectal cancer, nonmalignant $EGFR^+$ cells from the same patient organ were spared. This tumor-selective activity of Vγ9Vδ2 T cells appears to be an intrinsic beneficial feature of this cell type, though not previously reported using a tumor-targeting approach (44–46). Though incompletely understood, our data suggest that in the setting of EGFR-Vδ2 bsTCEs, this tumor preferential activity is at least in part related to differences in EGFR expression and interactions between NKG2D on Vγ9Vδ2 T cells and ligands thereof on tumor cells. In earlier work, we also demonstrated a modulatory role of phosphoantigen/BTN3A interactions by CD1d-Vδ2 bsTCE–engaged Vγ9Vδ2 T cells (21). Further research is required to assess the role of other Vγ9Vδ2 T cell–expressed receptors (e.g., DNAM-1 and NKG2A) in the observed tumor-selective reactivity.

Although the introduction of bispecific (pan) T-cell engagers has advanced cancer immunotherapy against hematologic malignancies (47), efficacy in solid tumors has thus far been disappointing. Toxicities such as CRS and neurotoxicity remain challenging in bsTCE-treated cancer patients (48) and their efficacy is hampered by cotriggering of immunosuppressive T-cell populations, such as Tregs, which dampen tumor-specific immune responses in a clinically relevant manner (16). We confirmed the negative impact of BiTE-induced Treg activation in both *in vitro* experiments, where EGFR-CD3 BiTEs significantly dampened Vγ9Vδ2 T-cell effector responses and proinflammatory cytokine production, as well as in patient colorectal cancer samples where EGFR-CD3 BiTEs stimulated highly suppressive activated Tregs. Specific activation of the proinflammatory effector Vγ9Vδ2 T-cell population with a bispecific Vγ9Vδ2 T-cell engager avoided such Treg coactivation.

Safety of targeting Vγ9Vδ2 T cells to EGFR was explored in NHP using 2 cross-reactive EGFR-Vγ9 bsTCEs, of which one was half-life extended by incorporation of an Fc domain. Previously, a CD3-based BiTE against EGFR demonstrated severe toxicity at doses of 31 and 154 μg/kg/day (continuous infusion), requiring termination of NHP after 56 hours for welfare reasons. In that study, NHP showed high cytokine release levels, signs of kidney and liver toxicity and histopathologic changes that included cell death in all tissues expressing EGFR (18). Even at over 2-log higher doses, EGFR-Vγ9-Fc bsTCEs did not trigger any clinical, biochemical or histopathologic signs of toxicity despite evidence of target engagement (i.e., binding of bsTCEs to PB and lymph node $V\gamma9^+$ T cells) and (postmortem) IHC confirmation of EGFR-Vγ9-Fc bsTCE presence in relevant tissues. In accordance with the absence of clinical signs, only minor changes in serum IL6 levels, a key regulator/mediator of CRS in patients treated with CAR T-cell and bsTCE therapies (49), were detected in EGFR-Vγ9 bsTCE-treated NHP. This further underscores the notion that EGFR-specific Vγ9Vδ2 T-cell engagers may combine strong antitumor efficacy with a relatively low risk of CRS and on-target, off-tumor toxicity and thereby potentially allow for a relatively large therapeutic window.

Altogether, and considering that EGFR is (over)expressed on a broad range of malignancies (32, 33), the here reported *in vitro*, *ex vivo*, and *in vivo* efficacy data against various $EGFR^+$ cancers together with the demonstrated benign safety profile in NHP, underscore the importance of exploring the antitumor potential as well as the safety profile of EGFR–Vγ9Vδ2 T-cell engagers in future clinical trials.

Authors' Disclosures

L.A. King reports grants from LAVA Therapeutics during the conduct of the study. M. Veth reports grants from LAVA Therapeutics during the conduct of the study. D. Amsen reports grants from Landsteiner Foundation for Blood Cell Research during the conduct of the study; personal fees from Abata outside the submitted work; in addition, D. Amsen has a patent for GPA33 as a marker for stable Tregs (2017) patent number 17163525.3 pending to Sanquinnovate. R. van de Ven reports personal fees from Genmab BV outside the submitted work. R.C. Roovers reports personal fees from LAVA Therapeutics during the conduct of the study. J.M. Ruben reports personal fees from LAVA Therapeutics during the conduct of the study. P.W. Parren reports personal fees and other support from LAVA Therapeutics NV during the conduct of the study; in addition, P.W. Parren has a patent for EGFR-Vdelta2 T-cell engagers licensed to Seagen and owned by LAVA Therapeutics. T.D. de Gruijl reports grants from LAVA Therapeutics NV during the conduct of the study; personal fees from LAVA Therapeutics NV and Mendus outside the submitted work; in addition, T.D. de Gruijl has a patent 10501540 licensed and with royalties paid from LAVA Therapeutics NV. H.J. van der Vliet reports grants and personal fees from LAVA Therapeutics during the conduct of the study; in addition, H.J. van der Vliet has a patent for WO15156673 issued and licensed to Seagen; and Dr van der Vliet is Chief Scientific Officer of LAVA Therapeutics. No disclosures were reported by the other authors.

Authors' Contributions

L.A. King: Conceptualization, resources, data curation, software, formal analysis, validation, investigation, visualization, methodology, writing–original draft, project administration, writing–review and editing. **E.C. Toffoli:** Writing–review and editing. **M. Veth:** Investigation, writing–review and editing. **V. Iglesias-Guimarais:** Formal analysis, visualization, writing–review and editing. **M.C. Slot:** Resources, investigation, writing–review and editing. **D. Amsen:** Resources, investigation, writing–review and editing. **R. van de Ven:** Resources, writing–review and editing. **S. Derks:** Resources, writing–review and editing. **M.F. Fransen:** Resources, writing–review and editing. **J.B. Tuynman:** Resources, writing–review and editing. **T. Riedl:** Writing–review and editing. **R.C. Roovers:** Investigation, methodology, writing–review and editing. **A.E.P. Adang:** Writing–review and editing. **J.M. Ruben:** Supervision, writing–review and editing. **P.W.H.I. Parren:** Resources, writing–review and editing. **T.D. de Gruijl:** Conceptualization, resources, supervision, investigation, methodology, writing–review and editing. **H.J. van der Vliet:** Conceptualization, resources, supervision, investigation, methodology, writing–original draft, writing–review and editing.

Acknowledgments

This research was funded by Lava Therapeutics NV, Utrecht, The Netherlands. M. C. Slot and D. Amsen were supported by a grant from the Landsteiner Foundation for Blood Cell Research (LSBR1818). The authors would like to thank the patients for participation, Tara Muijlwijk, Tessa van Schooten, Micaela Harrasser, Milon de Jong,

and Femke Burgers for their help with collecting patient material and information for Supplementary Table S1.

The publication costs of this article were defrayed in part by the payment of publication fees. Therefore, and solely to indicate this fact, this article is hereby marked "advertisement" in accordance with 18 USC section 1734.

Note

Supplementary data for this article are available at Cancer Immunology Research Online (http://cancerimmunolres.aacrjournals.org/).

Received February 27, 2023; revised April 4, 2023; accepted June 23, 2023; published first June 27, 2023.

References

1. Melandri D, Zlatareva I, Chaleil RAG, Dart RJ, Chancellor A, Nussbaumer O, et al. The γδ TCR combines innate immunity with adaptive immunity by utilizing spatially distinct regions for agonist selection and antigen responsiveness. Nat Immunol 2018;19:1352–65.
2. Harly C, Guillaume Y, Nedellec S, Peigne CM, Monkkonen H, Monkkonen J, et al. Key implication of CD277/butyrophilin-3 (BTN3A) in cellular stress sensing by a major human γδ T-cell subset. Blood 2012;120:2269–79.
3. Rigau M, Ostrouska S, Fulford TS, Johnson DN, Woods K, Ruan Z, et al. Butyrophilin 2A1 is essential for phosphoantigen reactivity by γδ T cells. Science 2020;367:eaay5516.
4. Pauza CD, Cairo C. Evolution and function of the TCR Vγ9 chain repertoire: It's good to be public. Cell Immunol 2015;296:22–30.
5. Kunzmann V, Bauer E, Feurle J, Weissinger F, Tony HP, Wilhelm M. Stimulation of γδ T cells by aminobisphosphonates and induction of antiplasma cell activity in multiple myeloma. Blood 2000;96:384–92.
6. Sawaisorn P, Tangchaikeeree T, Chan-On W, Leepiyasakulchai C, Udomsangpetch R, Hongeng S, et al. Antigen-presenting cell characteristics of human γδ T lymphocytes in chronic myeloid leukemia. Immunol Invest 2019;48:11–26.
7. Wrobel P, Shojaei H, Schittek B, Gieseler F, Wollenberg B, Kalthoff H, et al. Lysis of a broad range of epithelial tumour cells by human γδ T cells: involvement of NKG2D ligands and T-cell receptor- versus NKG2D-dependent recognition. Scand J Immunol 2007;66:320–8.
8. Gentles AJ, Newman AM, Liu CL, Bratman SV, Feng W, Kim D, et al. The prognostic landscape of genes and infiltrating immune cells across human cancers. Nat Med 2015;21:938–45.
9. Tosolini M, Pont F, Poupot M, Vergez F, Nicolau-Travers ML, Vermijlen D, et al. Assessment of tumor-infiltrating TCR Vγ9Vδ2 γδ lymphocyte abundance by deconvolution of human cancers microarrays. Oncoimmunology 2017;6:e1284723.
10. Cordova A, Toia F, La Mendola C, Orlando V, Meraviglia S, Rinaldi G, et al. Characterization of human γδ T lymphocytes infiltrating primary malignant melanomas. PLoS One 2012;7:e49878.
11. Todaro M, D'Asaro M, Caccamo N, Iovino F, Francipane MG, Meraviglia S, et al. Efficient killing of human colon cancer stem cells by γδ T lymphocytes. J Immunol 2009;182:7287–96.
12. Viey E, Fromont G, Escudier B, Morel Y, Da Rocha S, Chouaib S, et al. Phosphostim-activated γδ T cells kill autologous metastatic renal cell carcinoma. J Immunol 2005;174:1338–47.
13. Saura-Esteller J, de Jong M, King LA, Ensing E, Winograd B, de Gruijl TD, et al. Gamma Delta T-cell based cancer immunotherapy: past-present-future. Front Immunol 2022;13:915837.
14. Goebeler ME, Bargou RC. T cell-engaging therapies - BiTEs and beyond. Nat Rev Clin Oncol 2020;17:418–34.
15. Edeline J, Houot R, Marabelle A, Alcantara M. CAR-T cells and BiTEs in solid tumors: challenges and perspectives. J Hematol Oncol 2021;14:65.
16. Duell J, Dittrich M, Bedke T, Mueller T, Eisele F, Rosenwald A, et al. Frequency of regulatory T cells determines the outcome of the T-cell-engaging antibody blinatumomab in patients with B-precursor ALL. Leukemia 2017;31:2181–90.
17. de Bruin RCG, Veluchamy JP, Lougheed SM, Schneiders FL, Lopez-Lastra S, Lameris R, et al. A bispecific nanobody approach to leverage the potent and widely applicable tumor cytolytic capacity of Vγ9Vδ2-T cells. Oncoimmunology 2017;7:e1375641.
18. Lutterbuese R, Raum T, Kischel R, Hoffmann P, Mangold S, Rattel B, et al. T cell-engaging BiTE antibodies specific for EGFR potently eliminate KRAS- and BRAF-mutated colorectal cancer cells. Proc Natl Acad Sci U S A 2010;107:12605–10.
19. Honeywell RJ, Kathmann I, Giovannetti E, Tibaldi C, Smit EF, Rovithi MN, et al. Epithelial transfer of the tyrosine kinase inhibitors erlotinib, gefitinib, afatinib, crizotinib, sorafenib, sunitinib, and dasatinib: implications for clinical resistance. Cancers (Basel) 2020;12:3322.
20. Lameris R, de Bruin RC, van Bergen En Henegouwen PM, Verheul HM, Zweegman S, de Gruijl TD, et al. Generation and characterization of CD1d-specific single-domain antibodies with distinct functional features. Immunology 2016;149:111–21.
21. de Weerdt I, Lameris R, Ruben JM, de Boer R, Kloosterman J, King LA, et al. A bispecific single-domain antibody boosts autologous Vγ9Vδ2-T cell responses toward CD1d in chronic lymphocytic leukemia. Clin Cancer Res 2021;27:1744–55.
22. Opstelten R, de Kivit S, Slot MC, van den Biggelaar M, Iwaszkiewicz-Grzes D, Gliwinski M, et al. GPA33: a marker to identify stable human regulatory T cells. J Immunol 2020;204:3139–48.
23. Roovers RC, Vosjan MJ, Laeremans T, el Khoulati R, de Bruin RC, Ferguson KM, et al. A biparatopic anti-EGFR nanobody efficiently inhibits solid tumour growth. Int J Cancer 2011;129:2013–24.
24. de Bruin RCG, Lougheed SM, van der Kruk L, Stam AG, Hooijberg E, Roovers RC, et al. Highly specific and potently activating Vγ9Vδ2-T cell specific nanobodies for diagnostic and therapeutic applications. Clin Immunol 2016;169:128–38.
25. Goldstein NI, Prewett M, Zuklys K, Rockwell P, Mendelsohn J. Biological efficacy of a chimeric antibody to the epidermal growth factor receptor in a human tumor xenograft model. Clin Cancer Res 1995;1:1311–8.
26. Schmitz KR, Bagchi A, Roovers RC, van Bergen en Henegouwen PM, Ferguson KM. Structural evaluation of EGFR inhibition mechanisms for nanobodies/VHH domains. Structure 2013;21:1214–24.
27. Oberg HH, Peipp M, Kellner C, Sebens S, Krause S, Petrick D, et al. Novel bispecific antibodies increase γδ T-cell cytotoxicity against pancreatic cancer cells. Cancer Res 2014;74:1349–60.
28. Carter P. Bispecific human IgG by design. J Immunol Methods 2001;248:7–15.
29. Schutze K, Petry K, Hambach J, Schuster N, Fumey W, Schriewer L, et al. CD38-specific biparatopic heavy chain antibodies display potent complement-dependent cytotoxicity against multiple myeloma cells. Front Immunol 2018;9:2553.
30. Miyara M, Yoshioka Y, Kitoh A, Shima T, Wing K, Niwa A, et al. Functional delineation and differentiation dynamics of human CD4+ T cells expressing the FoxP3 transcription factor. Immunity 2009;30:899–911.
31. Middelburg J, Kemper K, Engelberts P, Labrijn AF, Schuurman J, van Hall T. Overcoming challenges for CD3-bispecific antibody therapy in solid tumors. Cancers (Basel) 2021;13:287.
32. Williet N, Petcu CA, Rinaldi L, Cottier M, Del Tedesco E, Clavel L, et al. The level of epidermal growth factor receptors expression is correlated with the advancement of colorectal adenoma: validation of a surface biomarker. Oncotarget 2017;8:16507–17.
33. Mendelsohn J. EGF receptors as a target for cancer therapy. Trans Am Clin Climatol Assoc 2004;115:249–53; discussion 53-4.
34. Lameris R, Ruben JM, Iglesias-Guimarais V, de Jong M, Veth M, van de Bovenkamp FS, et al. A bispecific T cell engager recruits both type 1 NKT and Vγ9Vδ2-T cells for the treatment of CD1d-expressing hematological malignancies. Cell Rep Med 2023;4:100961.
35. Nicol AJ, Tokuyama H, Mattarollo SR, Hagi T, Suzuki K, Yokokawa K, et al. Clinical evaluation of autologous gamma delta T cell-based immunotherapy for metastatic solid tumours. Br J Cancer 2011;105:778–86.
36. Wery-Zennaro S, Zugaza JL, Letourneur M, Bertoglio J, Pierre J. IL-4 regulation of IL-6 production involves Rac/Cdc42- and p38 MAPK-dependent pathways in keratinocytes. Oncogene 2000;19:1596–604.
37. Vantourout P, Hayday A. Six-of-the-best: unique contributions of gamma delta T cells to immunology. Nat Rev Immunol 2013;13:88–100.
38. Wakita D, Sumida K, Iwakura Y, Nishikawa H, Ohkuri T, Chamoto K, et al. Tumor-infiltrating IL-17-producing γδ T cells support the progression of tumor by promoting angiogenesis. Eur J Immunol 2010;40:1927–37.

39. Addison EG, North J, Bakhsh I, Marden C, Haq S, Al-Sarraj S, et al. Ligation of CD8α on human natural killer cells prevents activation-induced apoptosis and enhances cytolytic activity. Immunology 2005;116:354–61.
40. Ho LP, Urban BC, Jones L, Ogg GS, McMichael AJ. CD4(-)CD8αα subset of CD1d-restricted NKT cells controls T cell expansion. J Immunol 2004;172:7350–8.
41. Kadivar M, Petersson J, Svensson L, Marsal J. CD8αβ+ γδ T cells: a novel T cell subset with a potential role in inflammatory bowel disease. J Immunol 2016;197:4584–92.
42. Walker LJ, Kang YH, Smith MO, Tharmalingham H, Ramamurthy N, Fleming VM, et al. Human MAIT and CD8αα cells develop from a pool of type-17 precommitted CD8+ T cells. Blood 2012;119:422–33.
43. Wherry EJ. T cell exhaustion. Nat Immunol 2011;12:492–9.
44. Bryant NL, Suarez-Cuervo C, Gillespie GY, Markert JM, Nabors LB, Meleth S, et al. Characterization and immunotherapeutic potential of gammadelta T-cells in patients with glioblastoma. Neuro Oncol 2009;11:357–67.
45. Choudhary A, Davodeau F, Moreau A, Peyrat MA, Bonneville M, Jotereau F. Selective lysis of autologous tumor cells by recurrent γδ tumor-infiltrating lymphocytes from renal carcinoma. J Immunol 1995;154:3932–40.
46. Bouet-Toussaint F, Cabillic F, Toutirais O, Le Gallo M, Thomas de la Pintiere C, Daniel P, et al. Vγ9Vδ2 T cell-mediated recognition of human solid tumors. Potential for immunotherapy of hepatocellular and colorectal carcinomas. Cancer Immunol Immunother 2008;57:531–9.
47. Wu J, Fu J, Zhang M, Liu D. Blinatumomab: a bispecific T cell engager (BiTE) antibody against CD19/CD3 for refractory acute lymphoid leukemia. J Hematol Oncol 2015;8:104.
48. Yu J, Wang W, Huang H. Efficacy and safety of bispecific T-cell engager (BiTE) antibody blinatumomab for the treatment of relapsed/refractory acute lymphoblastic leukemia and non-Hodgkin's lymphoma: a systemic review and meta-analysis. Hematology 2019;24:199–207.
49. Shimabukuro-Vornhagen A, Godel P, Subklewe M, Stemmler HJ, Schlosser HA, Schlaak M, et al. Cytokine release syndrome. J Immunother Cancer 2018;6:56.